NASA Technical Memorandum 106705

Influence of Fiber Architecture on the Elastic and Inelastic Response of Metal Matrix Composites

Steven M. Arnold
Lewis Research Center
Cleveland, Ohio

Marek-Jerzy Pindera
University of Virginia
Charlottesville, Virginia

and

Thomas E. Wilt
University of Akron
Akron, Ohio

October 1995

National Aeronautics and
Space Administration

Trade names or manufacturers' names are used in this report for identification only. This usage does not constitute an official endorsement, either expressed or implied, by the National Aeronautics and Space Administration.

Influence of Fiber Architecture On The Elastic and Inelastic Response of Metal Matrix Composites

Steven M. Arnold
NASA-Lewis Research Center, Cleveland, OH 44135

Marek-Jerzy Pindera
University of Virginia, Charlottesville, VA

Thomas E. Wilt
University of Akron, Akron, OH 44235

Abstract

This three part paper focuses on the effect of fiber architecture (i.e., shape and distribution) on the elastic and inelastic response of metal matrix composites. The first part provides an annotative survey of the literature, presented as a historical perspective, dealing with the effects of fiber shape and distribution on the response of advanced polymeric matrix and metal matrix composites. Previous investigations dealing with both continuously and discontinuously reinforced composites are included. A summary of the state-of-the-art will assist in defining new directions in this quickly reviving area of research. The second part outlines a recently developed analytical micromechanics model that is particularly well suited for studying the influence of these effects on the response of metal matrix composites. This micromechanics model, referred to as the generalized method of cells (**GMC**), is capable of predicting the overall, inelastic behavior of unidirectional, multi-phased composites given the properties of the constituents. In particular, the model is sufficiently general to predict the response of unidirectional composites reinforced by either continuous or discontinuous fibers with different inclusion shapes and spatial arrangements in the presence of either perfect or imperfect interfaces and/or interfacial layers. Recent developments regarding this promising model, as well as directions for future enhancements of the model's predictive capability, are included.

Finally, the third part provides qualitative results generated using **GMC** for a representative titanium matrix composite system, SCS-6/TIMETAL 21S. Results

are presented that correctly demonstrate the relative effects of fiber arrangement and shape on the longitudinal and transverse stress-strain and creep response, with both strong and weak fiber/matrix interfacial bonds. The fiber arrangements include square, square diagonal, hexagonal and rectangular periodic arrays, as well as a random array. The fiber shapes include circular, square and cross-shaped cross sections. The effect of fiber volume fraction on the observed stress-strain response is also discussed, as is the thus-far poorly documented strain rate sensitivity effect. In addition to the well documented features of architecture dependent response of continuously reinforced two-phase MMCs, new results involving continuous multi-phase internal architectures are presented. Specifically, stress-strain and creep response of composites with different size fibers having different internal arrangements and bond strengths are investigated with the aim of determining the feasibility of using this approach to enhance the transverse toughness and creep resistance of TMCs.

Contents

1 INTRODUCTION

Developments over the past several years in the processing of advanced unidirectional metal matrix composites have provided new and exciting opportunities for tailoring the microstructure of these composites towards specific applications. Such tailoring may involve arranging the fibers into specific periodic arrays or distributions, and using fibers of more than one size, type, or shape. These new advancements in the processing and fabrication technologies (e.g. plasma spray and foil-groove techniques, etc.) now make it possible to truly engineer composite materials, propelling the composites community into a new era of materials development, analysis, and design. Examples of engineered materials include the concept of functionally graded materials, multi-phase composites with different types of reinforcement phases, and unidirectional metal matrix composites with engineered interfaces.

The emerging capabilities to engineer composite materials require the development of computationally efficient micromechanics approaches capable of predicting with sufficient accuracy the effect of microstructural details on the internal and macroscopic behavior of these materials. The computational efficiency is an indispensable requirement due to the large number of parameters that must be varied in the course of engineering a composite material. It is probably inevitable that the optimization of a material's microstructure will require the marriage of micromechanics models with optimization algorithms. From this perspective, analytical approaches that produce closed-form expressions which describe the effect of a material's internal architecture on the overall material behavior are preferable to numerical methods such as the finite-element or finite-difference schemes.

In this paper, a recently developed micromechanics analysis code (named **MAC**, see Wilt and Arnold, 1994) is employed to investigate the impact of continuous fiber architecture on the overall composite behavior under a variety of mechanical load histories. **MAC**'s predictive capability rests entirely upon the fully analytical micromechanics model, herein referred to as the generalized method of cells, **GMC**, (Paley and Aboudi, 1992; Aboudi and Pindera, 1992, Aboudi, 1994) which is capable of predicting the response of both continuous and discontinuous multi-phased composites with an arbitrary internal microstructure and reinforcement shape. **GMC** provides closed-form expressions for the macroscopic composite response in terms of the properties, size, shape, distribution, and response of the individual constituents or phases that make up the material. Details of **GMC** will be briefly outlined for completeness. Expressions relating the internal stress and strain fields in the individual constituents in terms of the macroscopically applied stresses and strains are also available through so-called strain or stress concentration factors. These expressions make possible the investigation of failure processes at the microscopic level at each step of an applied loading history, thus shedding light on how local damage affects the overall behavior, including macroscopic (ultimate) failure. Furthermore, **GMC** includes the capability to study the effect of debonding at the fiber/matrix interface which has been shown to be an important damage mechanism limiting the usefulness of silicon carbide/titanium (SiC/Ti) composites under transverse

and shear dominated loading (Karlak et al., 1974; Johnson et al., 1990; Nimmer et al., 1991a,b; Majumdar and Newaz, 1992; Lissenden et al. 1994).

In order to illustrate the need for a micromechanics-based model with the capabilities of **GMC**, a survey of literature dealing with the micromechanics modeling of the effects of fiber architecture, i.e. fiber shape and internal arrangement, on the overall composite response is first provided. This survey reveals that considerable work has been done during the early stage of composite material development in the 1960's and 1970's addressing the effects of fiber distribution, and to some extent fiber shape, on the internal stress and deformation fields, as well as the macroscopic elastic and inelastic behavior. It is important to note that the early modeling work, addressing the influence of fiber distribution on the macroscopic response, was carried out primarily in the context of attempting to identify the internal arrangements of circular cross-section fibers which yielded results that best fit the experimental data. These various investigations were partially motivated by the rapid development of small-diameter fiber composites such as glass/epoxy and graphite/epoxy wherein, the precise control of fiber distribution at the microscopic level is difficult, and only statistically macroscopic arrangements are possible. Similarly, in the case of early large-diameter fiber composites, such as boron/epoxy (B/Ep) and boron/aluminum (B/Al), the lack of technologies capable of precisely controlling fiber distributions was also a contributing factor. Notable exceptions include, the fundamental work of Drucker (1965) in which general principles were outlined that govern the strengthening of the elastoplastic response of particulate metal matrix composites through inclusion size, shape and distribution, and the modeling work of Foye (1966a,b), and Adams and Donner (1967a,b), aimed at investigating the effectiveness of fiber shape, as well as fiber arrangement, in strengthening the matrix. The results of these investigations were subsequently employed by Halpin and Tsai (1967) (see also Ashton, et al. (1969)) in developing design-oriented equations for predicting the elastic moduli of unidirectional composites with different fiber shapes and arrangements.

Recent investigations are characterized by more systematic studies of the effects of fiber geometry and distribution on the response of metal matrix composites, with the primary emphasis placed on the inelastic behavior. Due to the lack of tractable analytical approaches, the finite-element method typically has been employed by the various researchers. The results of such systematic computations make possible identification of rules governing the macroscopic behavior of metal matrix composites with different microstructures. These rules, in turn, can be useful both in explaining experimentally observed behavior and in designing composite materials with different microstructures. It is becoming increasingly clear, however, that more efficient approaches than the finite-element method are needed in developing a comprehensive set of guidelines for the design of a composite material's architecture. As mentioned previously, this is due to the large number of parameters that must be perturbed in identifying an optimal internal architecture. These parameters include material properties of the constituents since it is conceivable that an optimal fiber architecture for an elastoplastic matrix may no longer be optimal for a viscoplastic matrix where creep is dominant. The fact that **MAC/GMC**

is an accurate and efficient alternative tool for optimizing the microstructure of multi-phase metal matrix composites has been clearly demonstrated recently by Wilt (1995); wherein, a comparison between **GMC** and **FEM** unit cell analyses indicated that for the same transverse stress-strain response of a perfectly bonded composite, **GMC** requires *significantly* less CPU time, as illustrated in Fig. 1.

2 LITERATURE REVIEW

A variety of different micromechanical approaches have been employed in the past thirty years to study the overall behavior of composites from the knowledge of the properties of their constituents, geometry of the reinforcing phases and their distributions. A comprehensive and still relevant review of the different schemes for the elastic response has been offered by Chamis and Sendecky (1968), describing developments up to the late 1960's; whereas an outline of the different approaches for the elastoplastic response, including yielding, has been presented by Pindera (1983) which describes developments up to the late 1970's. Although progress in micromechanics has been made since then, the majority of work in micromechanical modeling of metal matrix composites is based on well-established numerical methods such as finite-element or finite-difference schemes. These numerical methods are currently employed to investigate specific problems in metal matrix composites which cannot be easily treated by the analytical approach. Notable exceptions include the development of the method of cells and its generalization (Aboudi, 1989, 1991; Paley and Aboudi, 1992; Aboudi and Pindera, 1992), the development of a new theory for functionally graded composites (Aboudi et al., 1993; 1994a,b; 1995), and the development of two analytical modeling schemes for periodic composites (Walker et al., 1989, 1991; Nemat-Nasser and Iwakuma, 1982; Nemat-Nasser and Hori, 1993). Mention also ought to be made of the homogenization theory, despite its finite-element based implementation, as it offers new perspectives for taking into account multi-directional loading of composites in a rational manner.

Only the methods (and their corresponding results) that have been employed to explicitly investigate the effects of fiber architecture on the overall composite response will be discussed herein. The references cited above will provide the reader with a more general outline of the various micromechanics schemes currently available. Review of the literature dealing with continuously reinforced composites is presented first, followed by review of the literature dealing with short-fiber, particulate and whisker reinforcement.

2.1 Continuous Fiber Composites

Review of the approaches used to predict elastic moduli is presented first since the results are also useful in understanding the initiation of yielding. The effectiveness of the reinforcement phase in controlling the subsequent plastic response can also be inferred from these models based on the knowledge of reported elastic stress fields. A

review of the elastic models also sheds light on the difficulty associated with the inelastic micromechanical analysis and explains the prevalent use of numerical approaches.

2.1.1 Micromechanical Modeling of the Elastic Response

Important results for the bounds on the elastic moduli of multi-phase composites with an arbitrary phase geometry have been established by Hashin and Shtrikman (1963) and Hashin (1965) using variational principles previously established by the authors. These bounds are valid for either a statistically homogeneous distribution of arbitrarily-shaped inclusions that produce macroscopically isotropic behavior, or a statistically homogeneous distribution of aligned transversely isotropic fibers of an arbitrary cross-section that produce macroscopically transversely isotropic behavior. Despite the fact that the differences between the lower and upper bounds may be significant depending on the mismatch in the elastic properties of the phases and the volume fraction, these bounds are useful in establishing the limits of possible maximization of the constituents' potential in so far as the properties of the constituent phases are concerned. These bounds are also useful in verifying the predictions of more detailed micromechanical approaches based on specific geometric models of the composite material's microstructure that produce macroscopically isotropic or transversely isotropic elastic moduli.

One such model is the composite cylinder assemblage (CCA) model in which the microstructure of a composite is modelled by an infinite array of composite cylinders of various sizes which completely fill the volume occupied by the composite material such that macroscopically uniform behavior is obtained (Hashin and Rosen, 1964; Hashin, 1972). Each composite cylinder consists of a fiber embedded in a surrounding matrix sheath such that the same fiber volume fraction for all cylinders is maintained. Under axisymmetric and axial shear loading, the behavior of the entire assemblage is the same as the behavior of a single composite cylinder which can easily be analyzed using standard analytical techniques. Unfortunately, only bounds on the transverse elastic moduli can be obtained, limiting the usefulness of the model. These bounds tend to be far apart for intermediate fiber volume fractions and large mismatches in the constituents' properties. Nevertheless, taken literally as a geometric model, the results can be compared with the results of periodic array models that will be discussed subsequently in order to determine the effect of a macroscopically uniform, but otherwise arbitrary, distribution of fibers of varying sizes on the overall elastic behavior.

Various elasticity solutions for different periodic distributions of inclusions or fibers have been obtained by numerous investigators by analyzing the response of a single repeating unit cell, or a basic building block of the array, under appropriate boundary and symmetry conditions that reflect the applied loading. Typically, the governing equations of elasticity are satisfied exactly while the continuity conditions between individual phases, and the boundary conditions on the unit cell, are satisfied approximately using point matching or least squares techniques. Application of this technique to determine the elastic moduli and internal stress distributions has been carried out by Pickett (1968),

and Leissa and Clausen (1968), using a Fourier series representation of the Airy's stress function in polar coordinates. Pickett considered regular distributions of circular fibers arranged in hexagonal and rectangular arrays, while Leissa and Clausen discussed extension of the method to fibers with elliptical and polygonal cross-sections without providing actual numerical results for the elastic moduli. Although no systematic comparison of the effect of fiber distribution on the elastic moduli has been provided by Pickett, his results nevertheless suggest that the transverse Young's moduli of a nearly square array of circular fibers are greater than those of a hexagonal array with the same fiber volume fraction (60%). The axial Young's modulus, on the other hand, was not significantly affected by the actual inplane fiber distribution and was suggested to be adequately predicted by the rule-of-mixtures approximation.

The finite-difference technique has been employed by Adams and Donner (1967a,b) to investigate the effects of material properties, fiber shape, spacing, volume fraction and periodic arrangement on the elastic response under longitudinal shear and transverse loading. Extensive results for the longitudinal shear moduli of unidirectional composites with circular, elliptical and square fibers in square and rectangular arrays were presented in graphical form. Also the effect of the considered parameters on the internal stress distributions was discussed with regard to localized yielding and failure. The dependence of the longitudinal shear modulus on the fiber shape for a rectangular array with equal fiber spacing in two principal directions was displayed graphically. Significant differences in the longitudinal shear modulus are observed at small filament spacings (i.e., large fiber volume fractions) for the considered fiber cross-sections for a B/Ep composite with a large shear modulus mismatch between fiber and matrix. However, these differences diminish as the fiber spacing increases (i.e., the fiber volume fraction decreases), and actually approaches at large fiber spacings the same limit, where little strengthening is observed . A square fiber cross-section produces the largest value of the longitudinal shear modulus, followed by an elliptical cross-section with the major axis in the plane of shear loading, followed by a circular cross-section, and finally by an elliptical cross-section with the major axis perpendicular to the loading plane. The maximum stress concentrations in the matrix follow the same trends, implying that localized failure may potentially negate the high strengthening effect of the inclusion at high concentrations unless relief through localized plastic flow is possible. Since the high stress concentrations are highly localized, effective strengthening of ductile elastoplastic matrices can be achieved using high concentrations of differently shaped fibers. The effect of periodic fiber arrangement on the longitudinal shear modulus of unidirectional composites with circular fibers was also presented for a wide range of fiber/matrix shear moduli ratios, showing that the square array produces a higher value than the hexagonal array, with the difference increasing substantially above fiber concentrations of 55 percent. An important result based on the comparison of the stress concentration factors in the matrix obtained from the periodic solution for a square and a rectangular array is that the nearby surrounding fibers tend to distribute the stresses more uniformly as the fiber spacing becomes more uniform in all directions, thus reducing the peak stresses.

The numerical results presented by Adams and Donner for the elastic response under transverse loading are not as extensive as those presented for the longitudinal shear problem. No information on the effect of fiber shape or periodic arrangement on the transverse elastic moduli is presented. Only limited results for the maximum normal stress in an equally spaced array of elliptical and circular fibers subjected to a uniform temperature change are given. These indicate that for a given fiber volume fraction, the elliptical fiber produces higher maximum normal stresses at the fiber/ matrix interface on the major axis than the square fiber, with the difference increasing with increasing aspect ratio of the ellipse.

Foye (1966a,b) used the finite-element technique to determine the elastic moduli of square, rectangular, diamond and hexagonal periodic arrays of fibers having various cross-sections. This is perhaps the first attempt to systematically study the effect of the fiber architecture on the elastic response of composites. The square array of circular fibers was shown to exhibit higher transverse Young's modulus than the hexagonal array, with the difference being small at low fiber concentrations and increasing substantially with increasing concentration for composites with large fiber/matrix modulus mismatch. The square array was much more conducive to high stress concentrations than the hexagonal array. The longitudinal shear modulus exhibited qualitatively similar trends, with substantially smaller differences between the square and hexagonal array values observed throughout the entire fiber volume fraction range, however. Comparison with the predictions of the CCA model revealed that the longitudinal shear modulus and the upper bound for the transverse Young's modulus were very close to the predictions of the hexagonal array. The transverse Young's modulus and the longitudinal shear modulus of elliptical and diamond shaped fibers with an aspect ratio of 4, calculated at a single value of the fiber volume fraction (0.3), were higher than the corresponding values for the circular fiber under loading parallel to the long dimension. The diamond fiber produced the highest moduli values and lowest stress concentrations. The influence of the aspect ratio of rectangular fibers on the transverse Young's modulus and longitudinal shear modulus was shown to be significant, with the cross-sections having the longer dimension in the plane of normal tension or shearing producing substantially higher values than the square geometry for a diamond array. Significantly smaller differences were obtained for the longitudinal shear modulus when the plane of shearing was aligned with the shorter dimension.

The results of Adams and Donner, and Foye, have been summarized by Ashton, et al. (1969), and compared with the design-oriented semi-empirical, semi-analytical micromechanics equations proposed by Halpin and Tsai (1967). The Halpin-Tsai equations use the rules-of-mixtures approximation for the longitudinal Young's modulus and Poisson's ratio irrespective of the fiber shape and distribution, which is partially justified based on the results of Pickett, and a common functional form for the remaining moduli. This common equation has been deduced from Hermans' (1967) generalization of the self-consistent model results and involves the fiber/matrix property ratio, fiber volume fraction and a geometric parameter that depends on the geometry of the inclusion, pack-

ing geometry and loading conditions. This geometric parameter must be determined from an appropriate solution to a given micromechanics problem. Comparison of the Halpin-Tsai predictions with selected results of Adams and Donner, and Foye, demonstrated the usefulness of the equations for design purposes.

In an attempt to explain the discrepancy between the transverse Young's modulus measured experimentally and predicted using micromechanics analysis based on the hexagonal fiber distribution, Adams and Tsai (1969) performed a finite-element analysis of square and hexagonal fiber arrays with quasi-random distributions. The square array has been included since it had been shown in previous investigations to correlate better with experimental data than the hexagonal array, contrary to intuition. Significantly better correlation was subsequently obtained between experimental data and the hexagonal random array, while introducing randomness into the square array resulted in poorer correlation.

2.1.2 Micromechanical Modeling of the Elastoplastic Response

Studies of initial yield surfaces using finite-element analysis were carried out by Lin et al. (1972a) for B/Al composites subjected to combined plane loading of longitudinal and transverse normal stresses, and inplane longitudinal shear stress. Yield surfaces for square-array geometries generated in the principal stress plane appeared to be convex and symmetric through the origin. It was observed that application of increasingly greater shear stresses caused the surfaces to shrink continuously. The above analyses were subsequently extended by the authors to the problem of longitudinal loading of unidirectional square-array B/Al and B/Ep laminae with the goal of determining the stress-strain response and progression of the elastic-plastic boundary (Lin et al., 1972b). The results indicated that initiation of yielding took place at opposite corners of the fiber/matrix interface closest to adjacent fibers and the plastic zone expanded very fast with increasing applied tractions. It was noted that the elastic limit macrostresses appeared to vary inversely with the matrix stiffness, while the ultimate tensile strength, as determined by local failure of either phase, depended on the elastic limits, Young's moduli, Poisson's ratios, and ductility of the materials.

Similar but more extensive studies were carried out by Dvorak et al. (1973, 1974) for unidirectional composites with hexagonal geometries subjected to arbitrary combinations of applied macroscopic stresses and temperature changes. In general the significant conclusions of these studies were that, yielding starts at the fiber/matrix interface for high fiber volume fractions; the plastic zone expands very fast with increasing macrostress, yield surfaces are convex; temperature changes can cause significant yielding and translation of the yield surface; composites yield under hydrostatic stress and exhibit volume changes; and yielding in the fiber direction is controlled by the fiber/matrix moduli ratio as well as the fiber volume fraction. High ratios inhibit yielding in the longitudinal direction, whereas yielding in the transverse plane is controlled by the matrix yield stress.

Also, high longitudinal and transverse shear stresses facilitate yielding under combined loads.

The presentation of the yield surfaces calculated by Lin and Dvorak for the square and hexagonal arrays does not lend itself to direct comparison in order to study the effect of the two fiber array geometries on initial yielding. Karlak and Crossman (1976), on the other hand, used the finite-element approach to study the effect of the fiber array geometry and fiber volume fraction on initial yielding in unidirectional B/Al composite under combined loading of the kind generated in an off-axis tension test. Square, square diagonal (diamond) and hexagonal arrays of circular fibers were analyzed under pure longitudinal and transverse loading, as well as combined loading involving longitudinal, transverse and inplane shear stresses varying according to the transformation equations with the fiber off-axis angle. Elastic moduli also were calculated for the different arrays and three fiber volume fractions ranging from 0.4 to 0.6. The results indicate that the longitudinal Young's and shear moduli, as well as the longitudinal yield strength were independent of the packing morphology. The transverse modulus and Poisson's ratios, on the other hand, were array morphology dependent, with the values for the hexagonal case approximately intermediate to the two square arrays. The transverse yield strength appeared to depend somewhat on the packing morphology, with slight differences between the square and hexagonal arrays, and somewhat greater observed differences between square and square diagonal arrays. For the fiber volume fraction of 0.4 and 0.5, the transverse yield strength of the square array was somewhat lower than that of the square diagonal array, whereas for the fiber volume fraction of 0.6 the reverse was true. Failure of the lamina through debonding when the interfacial normal stress at the fiber/matrix interface reached a certain percentage of the transverse yield strength was also investigated and found to be slightly dependent on the fiber array geometry. This was explained by noting the slight dependence of the lamina transverse yield strength on the fiber packing geometry.

Adams (1970) studied the inelastic response of B/Al and B/Ep composites under transverse loading, as a function of the fiber volume fraction and fiber arrangement. Square and rectangular arrays were considered and the results compared with experimental data. Progression of yielded zones was reported as a function of the applied transverse load, and nonlinear stress-strain curves were generated up to the initiation of local failure in either of the constituents. Significant differences were noted for the considered geometries. The rectangular array subjected to transverse tension in the direction of closer fiber spacing produced stiffer response and earlier initial failures than the corresponding square array due to the higher stress concentrations between closely-spaced adjacent fibers. Consequently, yielding was localized in the rectangular array, and thus the progression of yield zones more constrained relative to the square array which exhibited widespread yielding, producing significantly less ductile behavior prior to the initiation of first failure. Agreement with experimental data was found to be reasonable for the rectangular array but poor for the square one because the rectangular array more

closely resembled the actual fiber architecture. The effect of increasing the fiber volume fraction was to dramatically decrease the strain-hardening behavior.

Foye (1973) used the finite-element analysis based on the square-array geometry to study the transmission of constituent nonlinearities to the macroscopic behavior. The relevant observation from the viewpoint of the present survey is the small influence of the free-surface effect on the inelastic deformation. This observation was the result of comparing the response of a single row of fibers embedded in a strip of matrix with the corresponding results from the analysis of many such plies subjected to transverse normal loading. This single row of fibers produced a softer elastic response (as predicted by Hulbert and Rybicki (1971) in an earlier paper) than the configuration with many plies, which was not substantially magnified in the elastoplastic region. The stiffer response of the multi-ply configuration is due to the greater constraint of the adjacent fibers in the interior of the domain, which produces a higher triaxial state of internal stress. The stiffness decrease under longitudinal normal loading in a single ply was found to be considerably less than that in the multi-ply configuration; whereas under longitudinal shear loading the stiffness decrease was nonexistent. Note that yielding initiated at a point in the matrix midway between two adjacent fibers under transverse normal loading; whereas under longitudinal shear loading flow appeared to initiate at the fiber/matrix interface along the line of closest approach of adjacent fibers.

In a somewhat related investigation, Bigelow (1992) studied the effects of uneven fiber spacings in the surface plies and the interior, along with the fiber volume fraction, on the internal stress fields produced during fabrication cool-down of a SiC/Ti unidirectional composite. This was motivated by the experimental results of MacKay (1990) who reported radial microcracking in SiC/Ti unidirectional composites after processing. Substantially more microcracks were observed between closely spaced fibers than those with more uniform spacing. Surface plies exhibited more radial microcracking than in the interior. Not surprisingly, Bigelow found that the stress concentrations increased with decreasing fiber spacing, leading potentially to either radial microcracking or interfacial debonding in the case of touching fibers. Similar results were obtained for uneven fiber spacing in the surface plies, with somewhat greater values of peak stresses.

The effect of fiber array geometry on cracking susceptibility of ceramic matrix composites due to thermal expansion misfit was also investigated by Lu et al. (1991). The stress intensity factor for a radial crack emanating from a fiber/matrix interface was calculated as a function of the crack length for cubic and hexagonal arrays, as well as two fibers in an infinite matrix. The hexagonal fiber array was less susceptible to radial cracking than the cubic array. The greatest susceptibility to radial cracking was exhibited by two fibers in an infinite matrix, showing the deleterious effect of localized uneven fiber distributions in periodic arrays.

Wisnom (1990) investigated the effect of fiber array geometry on the inelastic response and failure of silicon carbide/aluminum (SiC/Al) unidirectional composites under transverse tension in the presence of a finite-strength interface and residual stresses. Rectangular and diamond arrays of circular cross-section fibers were investigated. Addi-

tionally, a ply composed of a single row of fibers was considered in order to compare the response of the surface ply with that of the interior plies. It was found that neither fiber array geometry nor fiber spacing, for the investigated geometries, affected the transverse strength when the primary mode of failure was interfacial failure, since the inability of the matrix to carry access load immediately resulted in total composite failure. In this scenario, the residual stresses play an important role delaying the average applied transverse stress which initiates localized debond failure. The reported data on the elastic moduli for the different fiber arrays indicated that the diamond fiber array produced the lowest value of the transverse Young's modulus, followed by the rectangular array with the long dimension parallel to the loading direction, and finally the rectangular array with the short dimension parallel to the loading direction. This result, of course, was consistent with the data reported long ago by Foye and others.

When interfacial debonding does not lead immediately to macroscopic failure of the composite, a substantially different conclusion is reached regarding the effect of the fiber array geometry. Nimmer et al. (1991a,b) investigated the response of a unidirectional SiC/Ti composite subjected to transverse loading using the finite-element approach based on a unit cell with three different aspect ratios, defined in terms of the unit cell dimensions in the plane of loading. A weak fiber/matrix interface was assumed that allowed debonding to occur when the fabrication-induced residual radial stress (which was compressive) was overcome by the externally applied transverse load. The initial elastic response of the three fiber arrays followed the trends established by earlier investigators. The rectangular array with the short unit cell dimension in the loading direction exhibited the stiffest response, followed by the nearly square array, and finally by the rectangular array with the long unit cell dimension parallel to the load direction. The small differences in the initial elastic response were substantially magnified when the interface was allowed to open up because of significant transfer of stress from the fiber to the matrix region in the plane perpendicular to the applied load. Since the fiber array with the long dimension along the loading axis possessed closely spaced fibers in the plane perpendicular to the load, the matrix in that plane supported a higher stress when debonding occurred than did the configuration with the short dimension along the loading axis. This stress magnification in the matrix phase between adjacent fibers in the plane perpendicular to the load direction, which is a function of the aspect ratio of the unit cell in the plane of loading, produced significant differences in the response of the different arrays when debonding occurred.

More systematic studies on the effects of fiber geometry and architecture have recently been provided by Brockenbrough et al. (1990, 1991) for a B/AL unidirectional composite under longitudinal and transverse tensile and shear loading. Elastic and inelastic response of square, hexagonal and circular fibers in square, square diagonal (a square array rotated by 45 degrees) and triangular (hexagonal array with equal fiber spacing) arrays was analyzed in the presence of a perfect bond using the finite-element approach. A random array of square and circular fibers was also included in the analysis based on a unit cell containing 26 and 30 fibers, respectively. No differences between the different

fiber arrays with different fiber shapes were observed for longitudinal loading; whereas substantial differences were observed for transverse tensile and shear loading. The significant conclusion (for transverse loading) was that fiber shape and fiber arrangement influence the inelastic response to a markedly greater extent than the elastic moduli. For instance, while a maximum variation of 17 percent in the elastic transverse Young's modulus was observed for the three different fiber arrangements with square, hexagonal and circular fibers, the variation in the inelastic response was substantially more dramatic, given a composite with a fiber volume fraction of 0.46. The extent of the variation in the inelastic region was shown to be a function of the fiber volume fraction, with smaller differences observed for low fiber volume fractions. The effect of the fiber array was much more pronounced than the effect of the fiber shape. For a given fiber shape (square or circular), the square array exhibited the stiffest elastic response and the greatest extent of strain hardening, followed by the random, triangular, and square diagonal arrays. The hexagonally shaped fiber in a triangular array produced an intermediate value of the elastic modulus and strain hardening. For a given fiber array, the square fiber produced a stiffer response in both the elastic and inelastic regimes than the circular fiber. The above results are directly related to the extent of stress triaxiality that develops in the different arrays with different fiber shapes. For instance, a square fiber in a square array produced a higher state of hydrostatic tension in the matrix, where plastic slip can occur, than a circular fiber in a square array (for the same applied average transverse stress). A hexagonal fiber in a triangular array produces a hydrostatic state of stress that lies between these two extremes.

The work by Brockenbrough et al. was extended by Nakamura and Suresh (1993) by including the effect of fabrication-induced residual stress on the response of unidirectional B/Al with circular fibers in square, square diagonal, hexagonal and random arrays. Residual stresses were sufficiently high to yield the matrix during simulated fabrication cool down, resulting in a slight reduction of the initial axial response in tension. The differences in the axial response of the various arrays were not significant, however. Thus residual stresses increased the composites resistance to plastic flow under transverse tension and reduced the strain hardening exponents of the considered fiber arrays; wherein the differences between strain hardening exponents for the different packing arrangements became significantly less pronounced given the presence of a residual stress field.

Kolle and Mueller (1991), and Mueller (1994) also investigated the response of unidirectional B/Al composite using the finite-element approach based on unit cells composed of a square fiber in a square array, and a circular fiber in square and hexagonal arrays. Results for all the thermo-elastic constants were presented for the different arrays at a low and a high fiber volume fraction. Little difference in the longitudinal Young's modulus, shear modulus, Poisson's ratio, and thermal expansion coefficients was seen between the different arrays, whereas, the differences in the transverse moduli were more substantial and became more pronounced with increasing fiber volume fraction. The differences in the elastoplastic response under transverse tension between the different arrays were also substantially more pronounced at higher fiber volume fraction. As reported by previous

investigators, the square array with a square fiber produced the stiffest response, followed by the square array with a circular fiber, and finally by the hexagonal array with a circular fiber.

The work of Bohm et al. (1993) based on the finite-element analysis of periodic arrays confirms the results for unidirectionally reinforced metal matrix composites with square and hexagonal array geometries reported by previous investigators, and also includes results on discontinuous fiber composites. A novel approach to generating finite-element representations for different arrangements of fibers allows efficient investigations of clustered arrays as well as perturbed periodic arrays. Of particular significance is the redistribution of microstresses in the perturbed arrays which may affect micro-level failure mechanisms by changing the hydrostatic and deviatoric components of the stress fields relative to those obtained for regularly spaced arrays.

2.1.3 Micromechanical Modeling of the Creep Response

Relatively little work has been done on the creep response of metal matrix composites with different fiber arrays and fiber shapes in comparison to the extensive work on the elastic and plastic tensile response. Crossman et al. (1974) were perhaps the first to study the effect of fiber array geometry on the creep response of unidirectional B/Al composites using the finite-element approach. Debonding of the interface was also included in the analysis. The work was conducted in order to develop equations for the steady-state creep of unidirectional composites as a function of fiber shape and geometry along similar lines as the Halpin-Tsai equations for the elastic moduli. The numerical results indicated that the transverse steady-state creep rate of a metal matrix composite reinforced by elastic fibers can be described in closed form by the same analytical creep relation used for the steady-state creep rate of the matrix with appropriate modifications for the geometry of the reinforcement and degree of debonding. These effects enter the steady-state creep rate equation for the composite through a geometric parameter. For example, given fully bonded composites with circular fibers, the transverse composite steady-state creep rate at a given stress level was highest for the diamond (or square diagonal) array, intermediate for the hexagonal, and the lowest for the square arrays. Alternatively, fully debonded composites exhibited significantly greater creep, and exhibited only slightly more creep resistance than material containing arrays of circular holes. Consequently, in the fully debonded case, the difference in the steady-state creep rate between the square and hexagonal arrays was significantly smaller than in the fully bonded case; the square array being slightly less resistant to creep than the diamond array.

In a follow-up investigation, Crossman and Karlak (1976) extended the uniaxial loading analysis to multi-axial loading. The primary conclusion was that for the considered material system, the longitudinal creep response was independent of the fiber array geometry (i.e., the transverse stresses created by the Poisson's ratio mismatch and geometric constraint of the various arrays did not contribute significantly to the axial creep), which led to the uncoupling of the longitudinal axial creep response from the longitudinal shear

and transverse responses. The effect of the fiber array geometry on the longitudinal shear creep response of fully bonded composites was found to be much less significant than under transverse loading. Although coupling between longitudinal shear and transverse loading was found to be substantial, and describable by simple interactive formulas, the reported results under combined loading were presented only for a square fiber array.

2.1.4 Continuous Fiber Composites Literature Summary

The various investigations described in the foregoing sections indicate extensive use of the numerical approach in studying the dependence of the effective composite response on fiber architecture. While the influence of fiber architecture on elastic moduli can potentially be studied in an efficient manner using the collocation technique originally employed by Pickett, as well as Clausen and Leissa, finite-difference and finite-element techniques were extensively employed to calculate elastic moduli for various fiber shapes and distributions as a function of the fiber volume fraction and the constituent property mismatch. Both fiber shape and distribution were demonstrated to influence the elastic moduli to varying degrees, depending on the direction of loading with respect to the fiber axis, fiber content, and fiber/matrix property mismatch. For normal loading parallel to the fiber direction, practically no dependence of the axial Young's modulus and Poisson's ratio on fiber architecture has been reported. Since this type of loading involves no direct stress transfer between the fiber and the matrix phases along the loading direction, the differences in the stress field caused by fiber architecture and Poisson's ratio mismatch in the plane perpendicular to the load (and fiber) axis are not sufficient to substantially influence the axial response. A different story emerges in the presence of direct stress transfer between the phases caused by transverse normal or shear, and axial shear loading. In this case, the fiber architecture may have a substantial effect on the associated elastic moduli, the extent of which depends on the fiber content and the fiber/matrix property mismatch. Work on the effect of fiber architecture on the response of discontinuous fiber composites reviewed in the following section aids in separating the relative influence of the fiber shape and fiber distribution, as well as in understanding the basic mechanisms associated with these variables. As will become apparent, the fiber shape directly influences the transfer of stress from the matrix to the fiber, while the fiber distribution plays a major role in controlling the extent of stress triaxiality in the matrix, thereby imposing a constraint on shearing deformation in the matrix. The effectiveness of these mechanisms in enhancing the elastic moduli of the composite increases with increasing fiber content and the fiber/matrix property mismatch.

When the matrix exhibits elastoplastic behavior, fiber architecture has a more significant influence on the elastoplastic response of the composite compared to the initial elastic behavior for transverse tensile and shear, as well as longitudinal shear, loading. The longitudinal elastoplastic response, on the other hand, is not affected by the fiber architecture as also observed in the elastic case. Since the fiber shape mainly controls local stress concentrations at the fiber/matrix interface, its effect on constraining plastic

deformation in the matrix tends to be localized. Alternatively, the fiber arrangement tends to provide constraint on plastic deformation throughout a substantially greater portion of the matrix at sufficiently large fiber concentrations. For this reason, the fiber arrangement appears to play a more important role in influencing elastoplastic response of the composite than the fiber shape.

Fiber arrangement also plays a substantial role in influencing the steady-state creep behavior of unidirectional composites. As in the case of the elastoplastic behavior, the longitudinal steady-state creep response is not affected by the fiber distribution, while under transverse loading substantial differences are observed between steady-state creep of square, hexagonal and diamond arrays of circular fibers. No data on the effect of fiber shape on the creep response appears to be presently available.

Tables I and II provide a summary (in chronological order) of those investigations discussed in the foregoing which provide explicit data on the effect of fiber architecture on the elastic, elastoplastic and creep response of continuously reinforced composites. While this summary indicates that a considerable amount of work has been done in the past to demonstrate and understand the effect of fiber architecture on the response of unidirectional composites, it should also be pointed out that this work, in general, has not been systematic or exhaustive. The reason for this is the predominant use of time-consuming finite-element analysis in modeling the response of composites with different shapes and fiber distributions. Thus the previous investigations often have focused on specific material systems, specific moduli or loading directions, limited ranges of fiber volume fractions, or specific inelastic or damage mechanisms. Very few investigations provide comprehensive data on the effect of both fiber shape and fiber distribution on the effective elastic, thermal and inelastic composite response. When such data is presented, it is typically restricted to one material system. Further, no data is available showing the effect of fiber architecture on the effective response of multi-phase composites (i.e., those with more than one type of fiber having different cross-sectional geometry and material properties).

The foregoing discussion reveals an abundant research area with a great potential for further investigation and exploitation. In particular, virtually no results are presently available demonstrating the effect of fiber architecture on the yield surfaces of unidirectional composites. The response to thermal loads also has not been investigated in sufficient detail in the presence of inelastic effects. The work involving inelastic matrix behavior has been limited primarily to classical incremental plasticity, as well as some steady-state creep, description of the matrix behavior. No unified viscoplasticity theories have been employed to model the rate sensitive response of the matrix phase under combined thermo-mechanical loading. Primary creep behavior for composites with different fiber architectures does not appear to have been investigated as well. The response of composites in the presence of damage is just beginning to be addressed, with the emphasis on interfacial debonding or failure. However, the evolution of damage in the matrix phase during creep or cyclic loading thus far has not been addressed. The above areas, together with extension of the investigations discussed in the foregoing to multi-phase

composites, open up new opportunities in this exciting new phase of composite material development and design.

2.2 Discontinuous Fiber Composites

The early work on the principles of strengthening in composites reinforced with discontinuous fibers, whiskers or particulates carried out in the 1950's and 1960's is characterized by the use of relatively simple models that do not explicitly take into account the actual inclusion distribution through interaction between adjacent fibers. These models have been employed to study the effect of inclusion shape on the elastic moduli, as well as subsequent inelastic response, and also the mechanism of stress transfer from the matrix to a finite-length fiber. For instance, Eshelby's analytical solution to the problem of an arbitrarily shaped ellipsoidal inclusion embedded in an homogeneous material deformed by uniform tractions or displacements at infinity has formed the basis for calculating the effective response of macroscopically homogeneous two-phase composites using a number of approaches (Eshelby, 1957). These approaches include the self-consistent scheme which neglects the inclusion/matrix interaction in calculating stress fields in the inclusion phase (Hill, 1965), and the Mori-Tanaka method which takes this interaction into account in an approximate fashion (Mori and Tanaka, 1973). The problem of an array of ellipsoidal inclusions with different aspect ratio embedded in an elastoplastic matrix can be treated using the Mori-Tanaka approach, as was done by Brown and Clarke (1975) in investigating the effect of inclusion shape on work hardening of metal matrix composites. However, this method typically underestimates yielding and subsequent hardening effects due to the use of mean stress and strain fields in the matrix phase, and treats all inclusion distributions on the same footing so long as macroscopic homogeneity is preserved. Along similar lines, the so-called shear-lag analysis has been employed to study the effectiveness of short fibers as reinforcement using the strength-of-materials approach to analyze stress fields around and within a finite-length fiber embedded in a surrounding matrix (Dow, 1963). While this type of analysis helps to identify shearing of the matrix as the primary mechanism of force transfer from the matrix to the fiber, and thus the critical fiber length over which the axial stress is introduced into the fiber from both ends, it is based on a very simplified one-dimensional analysis of stress fields which neglects the influence of morphology of surrounding fibers, among other things.

Despite the relatively long history of modeling the response of discontinuous fiber composites, only recently systematic investigations of the effects of reinforcement shape and arrangement have been initiated for these types of composites. Inclusion of the third dimension in the analysis of the elastic and inelastic response of discontinuous fiber composites increases the number of variables several fold relative to the analysis of continuous fiber composites. Thus, in addition to the arrangement and shape of the reinforcement in the plane transverse to the loading direction, variables associated with the planes parallel to the loading direction must be included. These variables include the fiber aspect ratio, fiber spacing in the vertical and horizontal directions, including

the effect of fiber clustering, and the extent of overlap between adjacent columns of fibers. The added complexity typically requires numerical solution procedures, such as the finite-elements analysis, if complicated reinforcement shapes and arrangements are involved.

The finite-element investigations carried out in recent years have focused on separating the effects of inclusion shape from the effects of inclusion array geometry on the overall elastic, elastoplastic and creep behavior. Examples of different inclusion shapes investigated include spherical particles, circular cylinders with different aspect ratios, truncated circular (octagonal) cylinders, double-cone particles, and ellipsoidal or disk-like particles. The different arrays studied include hexagonal arrangements of inclusions in the plane of loading distributed in either regular (aligned) arrays or off-set (staggered) arrays in the planes parallel to the loading direction. Inclusions such as disk-like particles arranged in packet morphologies have also been considered, as have clustered arrangements. These investigations have been driven in large part by the wide range of inclusion morphologies that result from current processing techniques, as well as by the wide range of shapes available for the inclusion phase.

In order to reduce the complexity of a three-dimensional finite-element formulation in analyzing the response of discontinuous fiber, whisker or particulate composites, various idealizations of the unit cell have been employed by a number of researchers (cf. Christman, et al., 1989; Tvergaard, 1990; Dragone and Nix, 1990; Povirk et al., 1990, 1992; Yang et al., 1991; Bao et al., 1991). For instance, in the case of a hexagonal array of inclusions in the plane transverse to the loading direction, the problem is often reduced to an axisymmetric (i.e., two-dimensional) problem by approximating the unit cell using a circular cylinder with different types of lateral boundary conditions to simulate the interaction with adjacent fibers (i.e., unit cells). Using this model, different fiber arrangements in the plane parallel to the applied load have been investigated, with varying amounts of overlap between vertical columns of adjacent fibers. The results of limited fully three-dimensional finite-element analyses of such periodic arrays are also available (Levy and Papazian, 1990), and these results support the general conclusions obtained from the simplified models. Alternatively, clusters of whiskers or cylindrical particles in the plane parallel to the applied load have been modeled using a plane strain idealization of rectangular platelets. This effectively reduces the problem to that of a continuously reinforced composite subjected to loading in the plane perpendicular to the long fiber direction. The results of such analysis for rectangular cross-sections with different aspect ratios in the plane of loading should be easily deduced from the early analysis of continuously reinforced composites with rectangularly shaped fibers discussed in the preceding sections (cf. Ashton et al., 1969).

Christman et al. (1989) employed the axisymmetric cell model with cylindrical and spherical inclusions arranged in a regular (non-staggered) array to study the effect of the inclusion and cell aspect ratio on the elastoplastic response of whisker and particulate reinforced metal matrix composites. The plane strain model was also employed to characterize the effect of whiskers clustering in the plane of loading on the overall and

local behavior. The development of triaxial stresses within the matrix due to constraint imposed by the reinforcement was shown to provide an important plastic strengthening contribution. These stresses are influenced by the inclusion shape and distribution, with the variation in the inclusion distribution in clustered arrays playing a greater role in the development of these stresses than the variation in whisker or cell aspect ratio in regular arrays. Since triaxial stresses are elevated in the vicinity of inclusion corners and are enhanced by plasticity, spherical inclusions are not as effective as cylindrical inclusions because the hydrostatic stress around spheres is not as large as around cylinders, thereby providing smaller constraint on the deformation. This explains why little strain-hardening is observed in composites reinforced by spheres at low inclusion concentrations relative to composites reinforced by particulates (i.e. unit cylinders) or whiskers (i.e. cylinders with aspect ratio greater than one). At low inclusion concentrations, the effect of clustering was found to be more important for whisker reinforced composites than particulate composites. Horizontal clustering (perpendicular to the load direction in the plane of loading) was shown to have no effect on the elastic modulus, while pronouncedly reducing the composite flow strength. This reduction was accompanied by a decrease in the triaxial stress state. Vertical clustering produced more dramatic reduction in the apparent flow strength than horizontal clustering.

The axisymmetric unit cell and plane strain models were also employed by Dragone and Nix (1990) to investigate the effect of reinforcement phase geometry on the creep response of discontinuous fiber metal matrix composites. The fiber volume fraction, fiber and unit cell aspect ratios, separation distance between adjacent fibers and the extent of fiber overlap (in clustered arrays) were shown to greatly influence the degree of constraint through development of triaxial stresses that control matrix flow, and ultimately to influence the overall composite deformation. For the same fiber concentration and aspect ratio, the aligned fiber composite (modeled by the axisymmetric unit cell) provided more constraint on the matrix deformation than the staggered array (modeled by the plane strain model of aligned platelets in the direction of loading), and resulted in lower creep strains. Based on the axisymmetric cell model, increasing both fiber and unit cell aspect ratio was more effective in reducing creep than increasing the fiber aspect ratio alone while keeping the inter-fiber distance constant. This is due to a higher degree of constraint achieved when the fiber spacing is allowed to decrease with proportionally increasing unit cell aspect ratio. Alternatively, increasing the side-to-side fiber spacing initially reduces the constraint on creep deformation, producing an increasing amount of creep until the effect of the decreasing fiber end-to-end spacing reverses the trend. The results of the plane strain model revealed that as the fiber overlap increased, greater hydrostatic stress and less shearing were produced in the matrix, and consequently the creep rate decreased.

A more accurate method of modeling staggered arrays was employed by Tvergaard (1990) using the axisymmetric, hexagonal array model with special boundary conditions to approximate the inclusion interaction. This approach better models the plastic shearing of the matrix between fiber ends in adjacent, vertically shifted fibers than the plane

strain model employed by other researchers. The effect of different periodic whisker patterns on the composite stress-strain response was investigated by varying the fiber and the cell aspect ratio, which control the fiber spacing and the extent of fiber overlap, together with the inclusion concentration. Relatively little influence of the cell aspect ratio was observed, which was explained by the competing effects of increasing overlap of adjacent fibers and increasing transverse spacing between adjacent fiber ends with decreasing cell aspect ratio. The effect of the fiber aspect ratio was substantially more pronounced than equivalent changes in the cell aspect ratio. The greatest effect on the macroscopic stress-strain response was due to variation in the inclusion volume fraction.

The axisymmetric unit cell model was also employed by Povirk et al. (1990) to study the effect of whisker spacing, aspect ratio and concentration on the evolution of residual stresses in regularly spaced (unstaggered) arrays. The side-to-side fiber spacing was concluded to be the most important parameter affecting the evolution of residual stresses and plastic matrix strains, while the fiber aspect ratio had little effect. This is because residual stresses were found to be independent of axial position a short distance from the fiber end. The plastic deformation was found to be confined to areas relatively close to the whiskers, and the volume of average plastic strains was primarily dependent on the whisker volume fraction with relatively little sensitivity to variation in the fiber and unit cell aspect ratios. Reduced residual compressive stresses were found in the areas of close side-to-side whisker spacing, thereby potentially promoting early void nucleation.

In a subsequent investigation, Povirk et al. (1992) employed the axisymmetric cell model to investigate the response of whisker and particulate metal matrix composites to mechanical loading in the presence of residual stresses due to a rapid quench. The modeling work was correlated with the results of neutron diffraction experiments from which residual elastic strains as a function of deformation were obtained. Parametric studies for the dependence of flow strength and residual strains on the fiber and unit cell aspect ratios, as well as fiber spacing and shape, were conducted in view of the lack of consistently quantitative correlation between theory and experiment. While the effect of the fiber aspect ratio on initial residual stresses was found to be small (as shown previously by the authors), the tensile flow strength and composite residual stresses after plastic deformation were influenced significantly by the fiber aspect ratio. The effect of the unit cell aspect ratio on flow strength was found to be smaller relative to the fiber aspect ratio. The flow strength increased with increasing fiber aspect ratio and increasing unit cell aspect ratio (decreasing side-to-side spacing, increasing end-to-end spacing). While thermal residual stresses were strongly affected by fiber spacing (as shown previously), fiber spacing was found to have a small effect on composite residual stresses after plastic deformation. Parametric studies involving cylindrical, ellipsoidal and conical reinforcement revealed that, for a fixed inclusion concentration, ellipsoidal inclusions produced the lowest proportional limit (lowest strengthening effect), while conical inclusions produced the highest. The asymptotic stress-strain behavior of a composite reinforced by cylindrical inclusions approached that of a composite reinforced by conical inclusions from below. The residual strains after plastic deformation were found to be substantially influenced

by inclusion shape, with conical reinforcement producing smallest deformation-induced residual stresses and cylindrical reinforcement highest.

Papazian and Adler (1990) conducted an experimental investigation on the strengthening effects of SiC particulates and whiskers on solution and precipitation hardened aluminum alloy matrix with different microstructures produced by aging. Not surprisingly, whiskers were found to be more effective than particulates in increasing the elastic modulus and strengthening the matrix against plastic flow. Increasing the whisker content produced a continuous increase in the elastic modulus, and an initial decrease in the proportional limit followed by an increase. The non-monotonic behavior of the proportional limit with increasing whisker content was suggested to be the result of two competing mechanisms, namely local stress concentrations at fiber ends and local constraint on the plastic deformation of the matrix due to adjacent fibers. The first mechanism dominates at low whisker concentrations, thereby initially lowering the proportional limit due to localizing yielding, while the second mechanism dominates at higher whisker concentrations, effectively constraining the plastic deformation in the matrix through development of high triaxial stresses as shown in a follow-up finite-element analysis. An important conclusion of the investigation was that for low inclusion concentrations (up to 20 percent), the flow behavior of the composite was more sensitive to matrix microstructure than to the addition of the SiC reinforcement.

In a subsequent investigation, Levy and Papazian (1990) conducted a three-dimensional finite-element analysis aimed at studying the effect of fiber and unit cell aspect ratio, and fiber distribution, on the effective stress-strain behavior of whisker reinforced composites. Both transversely aligned (unstaggered) and staggered arrays of cylindrical inclusions with a wide range of aspect ratios were investigated using a square packing arrangement in the plane perpendicular to the loading direction. For the unstaggered array subjected to longitudinal loading, increasing the fiber and unit cell aspect ratio in the same proportion at a fixed fiber concentration increased the effective elastic modulus, proportional limit, and work-hardening rate. For a fixed fiber and unit cell aspect ratio, both elastic modulus and work-hardening rate increased with increasing fiber concentration, while the proportional limit first decreased and then increased. These results duplicate the trends in the previously reported experimental data discussed above. Comparison of the staggered and unstaggered arrays at a fixed fiber concentration (20 percent) revealed that for low fiber and unit cell aspect ratios, the staggered array produces less work hardening and lower proportional limit, while for high aspect ratios the staggered array exhibits more work hardening and greater proportional limit. The differences between the staggered and unstaggered arrays diminish as the fiber aspect ratio is decreased. Comparison with experimental data revealed that a hybrid of the two models is required to accurately predict the initiation of yielding and subsequent hardening behavior of an aluminum alloy matrix containing 20 percent SiC whisker reinforcement. The results generated for both arrays subjected to transverse loading revealed a remarkable insensitivity of the transverse elastic properties and initial yield to variations in the fiber aspect

ratio. The work-hardening behavior under transverse loading was also not significantly affected by the fiber aspect ratio.

Bao et. al. (1991) employed the axisymmetric unit cell model to study the influence of inclusion shape, distribution and concentration on the flow strength of a ductile matrix reinforced by rigid inclusions. Uniform arrays of spheres, ellipsoidal and cylindrical inclusions in an elastic-perfectly plastic matrix were investigated using the unit cell model, and predictions for the flow strength of aligned ellipsoidal inclusions with different aspect ratios were compared to randomly oriented disc-like or needle-like particles arranged in a packet-like morphology. For an elastic-perfectly plastic matrix, little dependence of the flow stress on the concentration volume of spherical inclusions was observed in the dilute concentration range (up to 20 percent). Comparison of the flow stress for spherical particles with a three-dimensional cubic array analysis for concentration volumes up to 40 percent suggested that the flow strength is not significantly influenced by the actual regular distribution of spherical particles. Comparison of the flow strength for spherical, ellipsoidal and disk-like particles illustrated that the influence of the inclusion shape becomes increasingly significant with increasing aspect ratio and inclusion concentration. The needle-shaped inclusions were the most effective reinforcement against plastic flow, followed by disk-like particles and finally spheres. At low concentrations, the unit cell aspect ratio did not have a significant effect on the composite flow strength for spherical and disk-like reinforcement until particle spacing became small at which point the flow stress increased rapidly. Substantially more dependence of the flow strength on the unit cell aspect ratio was observed for the needle-shaped particles. Comparison of the composite flow strength for aligned needle-like and disk-like inclusions with randomly oriented needles and disks arranged in a packet-like morphology as a function of the inclusion concentration demonstrated that particle randomness destroys the shape advantage in aligned arrays. In particular, randomly oriented disks and needles produced similar results which were substantially lower than the corresponding results for aligned needle-like and disk-like particles, thus diluting the advantage of aligned needles over disks. Calculation of the flow strength for cylindrical reinforcement with different aspect ratios as a function of inclusion concentration revealed trends qualitatively similar to those observed for the ellipsoidal inclusions. The effect of the actual shape of the inclusion on the flow strength, however, was demonstrated to be substantial. For example, unit cylinders were twice as effective as spheres in increasing the composite flow strength at low inclusion concentrations. At higher aspect ratios, the difference between the effect of cylindrical shaped particles and ellipsoidal particles was less dramatic, but still appreciable.

Yang et al. (1991) conducted a carefully-controlled experimental investigation on Al-SiC composites reinforced with particulate inclusions and randomly oriented platelets, and compared the experimentally determined stress-strain response with that predicted by the approach of Bao et al. (1991). Generally good correlation between theory and experiment was obtained. The major conclusion supported the theoretical prediction that strengthening by equiaxed particles was approximately as effective as strengthening by randomly oriented platelets with a ten to one aspect ratio.

The problem of matrix cracking due to thermal expansion mismatch was investigated by Lu et al. (1991) as a function of the inclusion shape and size (and to a smaller extent fiber array geometry) in order to define under what conditions transverse matrix cracks and radial cracks emanating from a fiber/matrix interface could be suppressed. A critical reinforcement size was shown to exist below which matrix cracking is suppressed. A non-dimensional cracking coefficient, dependent on the misfit strain, matrix toughness and modulus, and reinforcement size, was successfully used to characterize cracking susceptibility of composites reinforced by different types of reinforcement.

In a sequence of papers, McHugh et al. (1993a-d) used an elastic-viscoplastic two-dimensional polycrystal finite-element model based on crystallographic slip theory to investigate the localization of plastic deformation as a function of inclusion morphology and volume fraction. The composite was modeled by an array of hexagonal grains reinforced by hexagonal inclusions arranged in several different morphological patterns. The authors found that the localization of plastic deformation evolved in patterns determined by the positions of reinforcing particles, and depended primarily on the inclusion volume fraction and morphology and less on the matrix hardening behavior. The effect of the morphology becomes more important with increasing inclusion volume fraction. Two of the patterns considered, rectangular and rhombus, had the same inclusion volume fraction making possible comparison of the influence of the inclusion array on plastic deformation. Under transverse loading the rectangular arrangement produced higher strain concentrations in the matrix near the inclusions, and lower strains elsewhere in the matrix, compared to the corresponding strains in the rhombus arrangement. Thus the rectangular arrangement provided a stronger constraint on plastic flow than the rhombus arrangement because a lower volume of the matrix was subjected to concentrated strain.

The influence of fiber architecture on the thermal expansion behavior of discontinuous fiber composites is still a relatively unexplored area. Siegmund et al. (1992) used the axisymmetric unit cell model to investigate the influence of unit cell aspect ratio on the axial thermal expansion response of staggered and non-staggered arrays at fixed fiber volume fraction and fiber aspect ratio. Varying the unit cell aspect ratio corresponds to moving fibers closer together in one direction and farther apart in the other. It was found that this variation had little effect on the axial thermal expansion of the staggered arrangement, but in the non-staggered arrangement larger unit cell aspect ratios (i.e., larger end-to-end and smaller side-to-side fiber spacing) lead to a significantly larger amount of thermal expansion.

In a more comprehensive investigation, Weissenbek and Rammerstorfer (1993) used the axisymmetric unit cell to investigate the influence of staggered (overlapping and non-overlapping) and non-staggered fiber arrangements on both mechanical and thermal expansion behavior of discontinuous fiber composites. A full three-dimensional unit cell model employed to validate the use of the axisymmetric approach confirmed the accuracy of the two-dimensional approach. The effect of residual stresses on subsequent thermal expansion and mechanical behavior was included in the calculations. While the global mechanical behavior of the composite was not strongly influenced by the inclusion ar-

rangement in contrast to the thermal expansion behavior, the local microstresses differed significantly in the investigated arrangements. Despite this, the evolution of damage based on matrix plastification did not lead to significant differences in the predicted failure stress for the different arrangements considered. This lack of difference was due to low sensitivity of the tensile stresses at the fiber ends that controlled failure on the fiber arrangement. Additional results on the response of discontinuous fiber composites with strong and weak interfaces in the presence of damage due to matrix plastification and interface failure using the above modeling approach and fiber arrangements have been presented by Abel et al. (1993).

Weissenbek et al. (1993) investigated the influence of inclusion shape and arrangement on the response of particulate-reinforced composites subjected to both mechanical and thermal loading. Both two-dimensional axisymmetric and three-dimensional unit cell models were employed. Spherical, cubical and unit cylindrical inclusions in simple cubic, face-center cubic and body-center cubic arrays were considered, along with unit cylinders in staggered and unstaggered square arrays. Substantially more strain-hardening was observed in the simple cubic arrangement of spherical inclusions than in the face-centered and body-centered cubic arrangements which both exhibited similar stress-strain response. This was due to the greater geometric constraint on the matrix deformation imposed by the simple cubic arrangement that produced higher hydrostatic matrix stresses relative to the other arrangements. For a given inclusion arrangement, the spherical inclusions produced substantially more compliant response than the unit cylindrical and cubical inclusions, which exhibited approximately the same amount of work hardening. In contrast to the mechanical response, the overall thermal expansion behavior of the three cubic configurations did not exhibit significant dependence on the particle arrangement.

Using the axisymmetric unit cell model, Shen et al. (1994) have performed extensive calculations to determine the elastic moduli of composites with uniformly distributed spherical, cylindrical, octagonal and conical inclusions. The plane strain model was also employed by the authors to investigate the dependence of elastic moduli on inclusion distribution. For a fixed inclusion aspect ratio, the conical inclusion produced the lowest value of the Young's modulus while the cylindrical inclusion the highest. The differences between the elastic moduli increased with increasing volume fraction of the inclusion, as well as increasing mismatch between the elastic properties of the inclusion and matrix phases. The differences observed were attributed to the differences in the load transfer capability for the investigated shapes. The results of the plane strain model revealed that the square array produced the stiffest response while the square diagonal array the softest. Square and square diagonal arrays with more than one inclusion size exhibited elastic moduli between these two extremes. The differences between the effective moduli for the different fiber distributions increased with increasing constituent property mismatch. These differences were attributed to the differences in the hydrostatic stress distributions which provided a constraint on the matrix shearing, thereby stiffening the elastic response for the distributions with a large hydrostatic stress component.

2.2.1 Discontinuous Fiber Composites Literature Summary

As in the case of continuously-reinforced composites, the investigations addressing the effect of inclusion architecture on the response of discontinuously-reinforced composites are characterized by predominant use of finite-element analysis of an idealized unit cell whose macroscopic behavior is representative of the composite. Due to many different types of reinforcement employed in discontinuously-reinforced composites, including whiskers, particulates, platelets as well as finite-length fibers, extensive analyses of inclusion shape have been conducted for this class of composites. Reinforcement shapes investigated include spheres, ellipsoids, cylinders of varying aspect ratios, truncated cylinders (octagons), cubes, platelets, and disk-like and needle-like inclusions. The different types of inclusion distributions that are possible in discontinuously-reinforced composites are typically modeled using two-dimensional axisymmetric unit cell models of hexagonal arrays in the plane perpendicular to the applied load, with different lateral boundary conditions that approximately model interaction between adjacent inclusions. Both unstaggered and staggered arrays parallel and perpendicular to the load axis in the plane of loading have been investigated in order to model and assess the influence of randomness that is typical of distributions in discontinuously-reinforced composites. Limited amount of data obtained with three-dimensional finite-element models generally supports the use of the two-dimensional axisymmetric unit cell models for the investigated fiber architectures. These models have been used to study the effect of inclusion shape and spacing on the composite response in periodic arrays. To investigate inclusion clustering effects in the plane of loading, plane strain models of inclusions with square cross sections have been employed that, in essence, do not differ from the analysis of continuous fiber composites under transverse plane strain loading.

In contrast with the work on continuously reinforced composites reviewed in Section 2.1, the investigations dealing with discontinuously-reinforced composites put a substantial emphasis on the reinforcement principles, the associated mechanisms, and how these mechanisms are affected by fiber architecture. As in the case of continuously-reinforced fibers under transverse load, the fiber architecture significantly affects the macroscopic response of discontinuously-reinforced composites through stress transfer from the matrix to the fiber, and through constraining the shearing deformation in the matrix phase. The fiber volume fraction naturally plays a significant role in controlling these mechanisms through the interaction between adjacent fibers.

Table III provides a summary of those investigations discussed in the foregoing which provide explicit comparison of the influence of the different fiber architectures on the response of discontinuously-reinforced composites. As is observed, the majority of investigations have focused on the inelastic response of these composites subjected to normal loads, with some recent attempts at systematically characterizing the influence of fiber architecture on the elastic moduli and to some extent damage.

2.3 Summary of Major Results and Future Perspectives

The literature survey presented in the foregoing sections indicates significant influence of both inclusion shape and distribution on the elastic, elastoplastic and creep response of continuous and discontinuous fiber composites. The extent of this influence for a given fiber architecture depends on the inclusion content, inclusion/matrix material property mismatch, and the direction of applied load with respect to the internal microstructure. For instance, the elastic, elastoplastic and creep response of continuously reinforced composites under longitudinal normal loading is virtually unaffected by fiber shape and fiber distribution, whereas substantial differences are observed in the transverse normal and shear, as well as longitudinal shear, response of composites reinforced by differently shaped fibers with different internal arrangements.

The work on discontinuously reinforced composites sheds light on the mechanisms at the micromechanics level that produce these shape- and distribution-dependent differences in the macroscopic composite response. Broadly speaking, the shape of an inclusion affects the stress transfer characteristics from the matrix to the fiber, which in turn render certain inclusion shapes more effective than others in reinforcing the matrix material. For this mechanism to play a role, the major loading component applied to the composite has to result in direct stress transfer between the phases. Since higher stresses are induced into square fibers under transverse loading than circular fibers, the transverse elastic moduli of composites continuously reinforced by square fibers are higher than those of circular fiber composites. The inclusion shape also directly influences the matrix stresses at and in the immediate vicinity of the inclusion/matrix interface. Inclusions with sharp corners produce high triaxial (hydrostatic) stresses at these locations, which locally constrain the extent of plastic strain evolution. Thus composites continuously reinforced with square fibers will exhibit higher yield stresses and hardening rates (and lower creep strains) under transverse loading than those reinforced by circular fibers. The extent of stress transfer and stress triaxiality for a given fiber shape increases with the fiber volume fraction and the material property mismatch between constituents. Consequently, differences in the response of continuously reinforced composites caused by differences in the fiber shape are small at low fiber volume fractions due to localized influence of non-interacting reinforcement and became more pronounced with increasing fiber volume fraction and material property mismatch.

The internal arrangement of inclusions, on the other hand, directly affects the distribution of stress triaxiality throughout the matrix phase which, in turn, constrains the magnitude of shear deformation under transverse loading and thus stiffens the matrix. This mechanism is more effective than the fiber shape in strengthening the matrix because its effect tends to be global rather than local at sufficiently high inclusion concentrations. For instance, a square array of fibers of a given cross-sectional shape will exhibit a stiffer response under transverse loading than a square-diagonal or hexagonal array of the same fibers because of higher hydrostatic stresses and lower shear stresses in the matrix.

The influence of fiber architecture on the composite response becomes more pronounced after initiation of yielding in the matrix phase. The differences in the magni-

tudes and distributions of hydrostatic stresses in the matrix caused by the differences in fiber architecture result in substantially different distributions and evolution rates of plastic strains. The plastic strain evolution is spatially nonuniform and nonproportional with respect to the externally applied loads, magnifying the differences in the response of composites with different architectures relative to their elastic response. As in the case of elastic moduli, these fiber architecture induced differences depend on fiber content, as well as fiber/matrix property mismatch.

The above observations briefly summarizing the influence of fiber architecture on the response of continuous and discontinuous fiber reinforced composites and are based on a substantial number of investigations, each of which was necessarily limited in scope due to the prevalent use of the finite-element approach in modeling the response of the investigated architectures. Thus while a considerable body of knowledge has been generated that sheds light on the effectiveness of different fiber architectures in strengthening continuous and discontinuous fiber composites, considerably more systematic research is required to develop design guidelines for optimization of material performance through fiber architecture manipulation. In particular, rate-dependent description of the matrix phase based on currently available unified viscoplasticity models has not been extensively employed in investigating the effects discussed in the foregoing. Incorporation of unified viscoplasticity models into micromechanical analyses of composites with different fiber architectures will make possible investigation of the effects of microstructural details on the composite response in a wide range of temperatures and loading rates, including rate-independent and rate-dependent stress-strain response, and primary, as well as steady-state, creep response. Investigation of the influence of fiber architecture on initial yielding under multi-axial loading is another area that has not been fully exploited. Considerably more work is also required in studying the effect of fiber architecture on the composite response in the presence of damage evolution in the individual phases. This includes such explicit mechanisms as fiber/matrix interfacial debonding, fiber or matrix cracking (either in the radial or transverse direction), and cavitation (cf. Ochiai and Osamura, 1989a,b; Zhenhai et al., 1991; Karbhari and Wilkins, 1991; Pagano and Brown, 1993). Incorporation of appropriate continuum-based models to describe gradual degradation of the matrix phase under thermo-mechanical fatigue loading in order to develop life-prediction guidelines is a related topic that remains to be broached. Clearly, each one of the above topics is relevant to multi-phase and functionally graded composites which are just beginning to be investigated.

It becomes clear, based on the above discussion, that in order to investigate the enumerated effects in an efficient and comprehensive manner, including parametric studies involving fiber content and material property mismatch variations, an approach other than the finite-element based micromechanics approach is required. This is particularly true when unified viscoplastic theories, which typically require computationally intensive integration algorithms, are employed to model the response of metallic matrices. The two-fold objective of the remainder of this paper is to, 1) illustrate that MAC/GMC is a micromechanics code ideally suited for both an accurate and efficient investigation

of the many different features of the macroscopic response of metal matrix composites with different fiber architectures and 2) to document the influence of fiber architecture on the inelastic (viscoplastic) behavior of MMCs. As the first step in meeting this objective, the previously documented features of continuously reinforced composites' behavior, characteristic of specific fiber architectures, are reproduced using **MAC/GMC**. Results are presented that correctly demonstrate the relative effects of fiber arrangement and fiber shape on the longitudinal and transverse stress-strain and creep response of a SCS-6/TIMETAL 21S[1] composite with a strong or weak fiber/matrix interfacial bond. Note that TIMETAL 21S is an advanced titanium-based matrix used in TMCs. The fiber arrangements include square, square diagonal, hexagonal and rectangular periodic arrays, as well as a random array. The fiber shapes include circular, square and cross-shaped cross-sections given a square packing arrangement. The effect of fiber volume fraction on the observed stress-strain response is included, as is the thus-far poorly documented strain rate sensitivity effect. In addition to the well-documented features of architecture-dependent response of continuously reinforced two-phase metal matrix composites, new results involving multi-phase internal architectures are presented. Specifically, stress-strain and creep response of composites with different-size fibers having different internal arrangements are investigated with the aim of determining the feasibility of using this approach to enhance toughness and creep resistance of metal matrix composites.

3 GENERALIZED METHOD OF CELLS

The generalized method of cells is a recent and natural extension of a micromechanics model, known in the literature as the method of cells (**MOC**), which was developed by Aboudi (1989, 1991) for predicting the response of metal matrix composites and will now be briefly summarized. In the original formulation of **MOC**, a continuously (or discontinuously) reinforced composite is modeled as a doubly (or triply) periodic array of fibers or inclusions embedded in a matrix phase. The periodic character of the assemblage allows one to identify a repeating unit cell that can be used as a building block to construct the entire composite. The properties of this repeating unit cell are thus representative of the properties of the entire assemblage. The unit cell consists of a single fiber (or inclusion) subcell embedded in three matrix subcells for continuous, and seven matrix subcells for discontinuous composites, hence the name **method of cells**. The Cartesian geometry of the repeating unit cell allows one to obtain an approximate solution for the stresses and strains in the individual subcells given some macroscopically homogeneous state of strain or stress applied to the composite. The approximate solution to the thus posed boundary-value problem is, in turn, used to determine macroscopic (average) or effective properties of the composite and the effective stress-strain response in the inelastic region.

[1]TIMETAL 21S is a registered trademark of TIMET, Titanium Metals Corporation, Toronto, OH.

Although **MOC** has been demonstrated in numerous experimental/analytical correlation studies to be an accurate and, at the same time, efficient tool for analyzing the inelastic response of metal matrix composites over a wide temperature range, it suffers from several drawbacks. The use of four (or eight) subcells limits the analysis of continuous (or discontinuous) MMC's to essentially two-phase composites with a limited number of fiber or inclusion arrays. Only regular arrays with, at most, two different fiber spacings or three inclusion spacings can be analyzed by the original method. This sparse discretization of the unit cell also precludes the possibility of including an interfacial region between the fiber and the matrix phases, as well as considering more complicated (or refined) fiber shapes. The transversely isotropic behavior of unidirectional composites in the plane perpendicular to the fiber direction is imposed artificially by equating the unit cell dimensions in the plane perpendicular to the fiber direction and subsequently averaging out the effect of the square geometry of the unit cell. These limitations motivated the development of the generalized method of cells or **GMC**.

In the **generalized** formulation for continuous (or discontinuous) multiphased composites, the repeating unit cell is subdivided into an arbitrary number of subcells or phases. Hence this generalization extends the modelling capability of the original method of cells to include the following: 1) inelastic thermomechanical response of multi-phase, metal matrix composites, 2) modelling of various fiber (phase) architectures including both shape and packing arrangements, 3) modelling of porosities and damage, and 4) the modelling of interfacial regions around inclusions, including interfacial degradation.

The basic homogenization approach taken in the micromechanical analysis consists essentially of four steps. First, the representative volume element, RVE, (or repeating unit cell) of the periodic composite is identified. Second, the macroscopic or average stress and strain state in terms of the individual microscopic (subcell) stress and strain states is defined. Third, the continuity of tractions and displacements are imposed at the boundaries between the constituents. These three steps, in conjunction with micro-equilibrium, establish the relationship between micro (subcell) total, thermal, and inelastic strains and macro (composite) strains via the relevant concentration tensors. In the fourth and final step, the overall macro constitutive equations of the composite are determined. These four steps form the basis of the micro-to-macro mechanics analysis which describe the behavior of heterogeneous media (Aboudi, 1989 and 1994). The resulting micromechanical analysis establishes the overall (macro) behavior of the multi-phase composite and is expressed as a constitutive relation between the average stress, and total, thermal, and inelastic strains, in conjunction with the effective elastic stiffness tensor.

Thus, the average stress is represented as,

$$\bar{\sigma} = \boldsymbol{B}^*(\bar{\epsilon} - \bar{\epsilon}^I - \bar{\epsilon}^T) \tag{1}$$

where for the most general case of discontinuous reinforcement with N_α by N_β by N_γ number of subcells (see Fig. 2), the effective elastic stiffness tensor, $\boldsymbol{B}^*$, of the composite is given by,

$$B^* = \frac{1}{dh\ell} \sum_{\alpha=1}^{N_\alpha} \sum_{\beta=1}^{N_\beta} \sum_{\gamma=1}^{N_\gamma} d_\alpha h_\beta \ell_\gamma C^{(\alpha\beta\gamma)} A^{(\alpha\beta\gamma)} \tag{2}$$

and the composite inelastic strain tensor is defined as,

$$\bar{\epsilon}^I = \frac{-B^{*-1}}{dh\ell} \sum_{\alpha=1}^{N_\alpha} \sum_{\beta=1}^{N_\beta} \sum_{\gamma=1}^{N_\gamma} d_\alpha h_\beta \ell_\gamma C^{(\alpha\beta\gamma)} (D^{(\alpha\beta\gamma)} \epsilon_s^I - \bar{\epsilon}^{I(\alpha\beta\gamma)}) \tag{3}$$

and the average thermal strain tensor as

$$\bar{\epsilon}^T = \frac{-B^{*-1}}{dh\ell} \sum_{\alpha=1}^{N_\alpha} \sum_{\beta=1}^{N_\beta} \sum_{\gamma=1}^{N_\gamma} d_\alpha h_\beta \ell_\gamma C^{(\alpha\beta\gamma)} (D^{(\alpha\beta\gamma)} \epsilon_s^T - \bar{\epsilon}^{T(\alpha\beta\gamma)})) \tag{4}$$

and ϵ is the uniform applied macro (composite) strain. For the case of continuous reinforcements with N_α by N_β number of subcells, eqs. (2) - (4), reduce to the following:

$$B^* = \frac{1}{h\ell} \sum_{\beta=1}^{N_\beta} \sum_{\gamma=1}^{N_\gamma} h_\beta \ell_\gamma C^{(\beta\gamma)} A^{(\beta\gamma)} \tag{5}$$

$$\bar{\epsilon}^I = \frac{-\mathrm{B}^{*-1}}{h\ell} \sum_{\beta=1}^{N_\beta} \sum_{\gamma=1}^{N_\gamma} h_\beta \ell_\gamma C^{(\beta\gamma)} (D^{(\beta\gamma)} \epsilon_s^I - \bar{\epsilon}^{I(\beta\gamma)}) \tag{6}$$

$$\bar{\epsilon}^T = \frac{-\mathrm{B}^{*-1}}{h\ell} \sum_{\beta=1}^{N_\beta} \sum_{\gamma=1}^{N_\gamma} h_\beta \ell_\gamma C^{(\beta\gamma)} (D^{(\beta\gamma)} \epsilon_s^T - \bar{\epsilon}^{T(\beta\gamma)})) \tag{7}$$

In the above equations matrix notation is employed; where, for example, the average stress $\overline{\sigma}$,average applied strain, $\bar{\varepsilon}$, and inelastic subcell strain, ε_s^I, vector represent,

$$\overline{\sigma} = (\overline{\sigma}_{11}\ ,\ \overline{\sigma}_{22}\ ,\overline{\sigma}_{33}\ ,\ \overline{\sigma}_{23}\ ,\ \overline{\sigma}_{13}\ ,\ \overline{\sigma}_{12}) \tag{8}$$

$$\bar{\epsilon} = (\bar{\epsilon}_{11}\ ,\ \bar{\epsilon}_{22}\ ,\ \bar{\epsilon}_{33}\ ,\ 2\bar{\epsilon}_{23}\ ,\ 2\bar{\epsilon}_{13}\ ,\ 2\bar{\epsilon}_{12}) \tag{9}$$

$$\epsilon_s^I = (\bar{\epsilon}^{I(111)}, \ldots, \bar{\epsilon}^{I(N_\alpha N_\beta N_\gamma)}) \tag{10}$$

where the six components of the vector $\bar{\epsilon}^{I(\alpha\beta\gamma)}$ are arranged as in eq. (8). Similar definitions for ϵ_s^T ,$\epsilon^{T(\alpha,\beta,\gamma)}$ also exist. Note that the key ingredient in the construction of this macro constitutive law is the derivation of the appropriate concentration matrices, $\mathrm{A}^{(\alpha,\beta,\gamma)}$ and $\mathrm{D}^{(\alpha,\beta,\gamma)}$ having the dimensions 6 by 6 and 6 by $N_\alpha N_\beta N_\gamma$ respectively, at the micro (subcell) level. The definitions of A and D, although not given here, may be found in Paley and Aboudi (1992), and Aboudi (1994). Finally, $\mathrm{C}^{(\alpha,\beta,\gamma)}$ represents the elastic stiffness tensor of each subcell $(\alpha\beta\gamma)$ and $d_\alpha, h_\beta, \ell_\gamma$ the respective subcell dimensions (see Fig. 2) wherein,

$d = \sum_{\alpha=1}^{N_\alpha} d_\alpha$ $\qquad$ $h = \sum_{\beta=1}^{N_\beta} h_\beta$ $\qquad$ $\ell = \sum_{\gamma=1}^{N_\gamma} \ell_\gamma$

Similarly, given the concentration matrices $\mathbf{A}^{(\alpha,\beta,\gamma)}$ and $\mathbf{D}^{(\alpha,\beta,\gamma)}$, expressions for the average strain in each subcell can be constructed, i.e.,

$$\epsilon_s = A\bar{\epsilon} + D(\epsilon_s^I + \epsilon_s^T) \tag{11}$$

as well as average stress,

$$\bar{\sigma}^{(\alpha\beta\gamma)} = C^{(\alpha\beta\gamma)} \left[A^{(\alpha\beta\gamma)}\bar{\epsilon} + D^{(\alpha\beta\gamma)}(\epsilon_s^I + \epsilon_s^T) - (\bar{\epsilon}^{I(\alpha\beta\gamma)} + \bar{\epsilon}^{T(\alpha\beta\gamma)}) \right] \tag{12}$$

The analytic constitutive law, see eq. 1, may be readily applied to investigate the behavior of various types of composites, given a knowledge of the behavior of the individual phases. Numerous advantages can be stated regarding the current macro/micro constitutive laws as compared to the other numerical micromechanical approaches in the literature, e.g. the finite element unit cell approach. One advantage is that any type of simple or combined loading (multiaxial state of stress) can be applied irrespective of whether symmetry exists or not, as well as without resorting to different boundary condition application strategies as in the case of the finite element unit cell procedure. Another advantage concerns the availability of an analytical expression representing the macro elastic-thermoinelastic constitutive law thus ensuring a reduction in computational costs and memory requirements when implementing this formulation into a structural finite element analysis code. Similarly, this formulation admits a wide variety of physically based deformation (e.g. unified associative and nonassociative viscoplastic models) and life models. Furthermore, this formulation has been shown to predict accurate macro behavior given only a few subcells within the repeating cell (see Paley and Aboudi (1992), Arnold et al. (1993) and Wilt (1995)). Alternatively, if one employs the finite element unit cell procedure, a significant number of finite elements are required within a given repeating unit cell to obtain the same level of accuracy as with the present formulation, see Fig. 1. Consequently, it is possible to utilize this formulation to efficiently analyze metal matrix composite structures subjected to complex thermomechanical load histories. This is particularly important when analyzing realistic structural components, since different loading conditions exist throughout the structure and thus necessitate the application of the macromechanical equations repeatedly at these locations.

As mentioned previously, the computationally efficient and comprehensive micromechanics analysis code, **MAC**, whose predictive capability rests entirely upon the above described generalized method of cells, was used to obtain all of the results given in the next section. **MAC** enhances the basic capabilities of **GMC** by providing a modular framework wherein 1) various thermal, mechanical (stress or strain control) and thermomechanical load histories can be imposed, 2) different integration algorithms may be selected, 3) a variety of constituent constitutive model may be utilized and/or implemented and 4) a variety of fiber architectures may be easily accessed through their corresponding representative volume elements. The capabilities of **MAC** version 1.0 used to generate the subsequent results are documented in Wilt and Arnold (1994).

4 MAC/GMC RESULTS

The results presented herein will be limited to continuously reinforced composites. Although the three-dimensional version of **GMC** recently developed by Aboudi (1994) can be employed to efficiently investigate the influence of fiber architecture on the response of short-fiber, whisker or particulate composites reviewed in Section 2.2, this will be reserved for future work. The subsequent results are all qualitative in nature, in that no attempt was made to 1) include any residual stresses induced during processing and 2) calibrate the weak interface to be representative of the actual composite system's transverse response. The primary objective of this study is to qualitatively assess the impact of fiber architecture on the inelastic behavior of MMCs and to demonstrate that **MAC/GMC** is fully capable of analyzing the wide variety of architectural effects discussed in the literature and more. To this end it is imperative that an accurate multiaxial viscoplastic model representing the inelastic behavior of the titanium matrix (TIMETAL 21S) be utilized. The fully associative, nonlinear kinematic hardening, generalized viscoplastic with potential structure (**GVIPS**) model put forth by Arnold et al. (1994, 1994a,b, and 1995) has been shown to accurately capture the history dependent deformation response (e.g. rate sensitivity, creep and relaxation) of TIMETAL 21S over a wide temperature range. However, in this study all analyses were conducted at 650°C (or 1200°F). Finally, unless otherwise specified a pseudo square fiber idealization is utilized for all architectures, wherein the Young's modulus, Poisson ratio, and coefficient of thermal expansion for the SCS-6 fiber were taken as E = 400 GPa, $\nu = 0.32$, $\alpha = 2.1x10^{-6}/\ ^{\circ}C$, respectively.

4.1 Tensile Behavior

Let us begin by examining the qualitative tensile behavior of a 35 percent volume fraction, square fiber array, SCS-6/TIMETAL 21S composite system. Figure 3 shows the constituent (i.e., fiber and matrix), and, predicted longitudinal and transverse composite stress-strain response of this system. As expected, the longitudinal response exhibits a bi-linear stress-strain response whereas the transverse response, be it strongly or weakly bonded, exhibits a nonlinear stress-strain response similar to that of the matrix material (TIMETAL 21S) alone. Note that the strongly bonded transverse response is above (whereas, the weakly bonded response falls below) the neat (fiber-less) matrix response, thus capturing the qualitative experimentally observed behavior.

The imperfect or weakly bonded response illustrated in Fig. 3 can be simulated in **MAC/ GMC** by either imposing some type of interface discontinuity condition at the subcell boundaries (Aboudi (1988), Robertson and Mall (1993) and (1994)) or explicitly defining an interface subcell with a finite thickness and its own constitutive response, Aboudi (1993). The latter option was used here for all weakly bonded, transverse response analyses performed; wherein the interface material comprised 10 percent of the total volume fraction of the material. Note, although this idealization is not completely consistent with the physics of the interfacial failure (in that, stress concentrations at the

point of interfacial separation are not induced), such an idealization adequately captures, for deformation analysis purposes, the softening influence of the fiber/matrix interfacial debonding. Also, this idealization is consistent with the approximate formulation of GMC in that equilibrium and continuity are satisfied in an average sense, and thus GMC would not be able to detect such a localized feature as stress concentrations at a crack tip. Furthermore, an advantage to utilizing an interfacial layer, instead of interfacial discontinuity conditions, resides in the consistent coupling of the multiaxial stresses and differences in tension and compression behavior which are handled via the interfacial constitutive model.

To illustrate the influence of various interfacial constitutive models on the transverse composite behavior, two types of interface models were assumed. The first was a purely elastic model where the Young's modulus of the interface was assumed to be 10% and 1% respectively of the matrix modulus. The resulting stress-strain responses are shown in Fig. 4. Note, how the initial effective modulus is significantly influenced by the presence of this interface region and how even under the slightest transverse tensile load the stress-strain response deviates immediately (as no compressive residual stress state is present) from that of the strongly bonded case. Although this elastic interface region produces a macro response that is not consistent with experimental observations, other researches using a similar idealization have documented this type of result. Alternatively, an experimentally consistent macro response is achievable when an interfacial layer material is introduced whose constitutive response is identical to that of TIMETAL 21S (the matrix) except that its flow property resembles that of a perfectly viscoplastic material. This interface constituent response (line ab) is shown in Fig. 4 along with the associated weakly bonded composite (macro) response (line ac). Clearly, this transverse stress-strain response possesses qualitatively the three experimentally observed deformation regions, see Majumdar and Newaz (1992), and, Lerch and Saltsman (1993). That is, an initial elastic region that corresponds to the strongly bonded case (when the interface is closed), a slightly nonlinear region that is associated with the opening of the interface, and finally a highly nonlinear region associated with interface opening and matrix inelasticity. Note, with such an idealization the interfacial yield stress now becomes the calibration parameter that will dictate the point at which the transverse composite response deviates from the strongly bonded case.

In order to demonstrate the versatility of MAC and the influence of volume fraction and fiber array packing (geometry) on the transverse tensile response, three fiber volume fractions (i.e., 20, 35 and 50%), five fiber packing arrays, depicted in Fig. 5, and both strong and weak interfacial conditions were examined. Additionally, a random packing arrangement was analyzed for the strongly bonded, 35 percent volume fraction case. The response curves illustrates the composite transverse response for fiber volume fractions of 20, 35 and 50 percent are shown in Figs. 6, 7, and 8, respectively. Clearly, the results indicate a significant influence of packing geometry on the transverse response with this influence increasing dramatically at higher volume fractions, particularly in the case of a strongly bonded system. Specifically, at a volume fraction of 20%, there is

very little difference between packing geometries whereas at a 50% volume fraction the difference in each packing geometry is clearly distinguishable due to the increased fiber interaction. The various trends in Figs. 6, 7 and 8 are consistent with those discussed in the literature. For example, the rectangular packing arrangement with high R ratio (ratio of horizontal to vertical distance between inclusion phases) exhibited the stiffest tensile response, followed by the rectangular (R=0.74), square, hexagonal, and the square diagonal giving the least stiff tensile response (see Table II for various literature references). This array ordering is independent of bond strength as it is primarily associated with the enhancement or reduction of a triaxial (i.e., hydrostatic) stress state in the matrix, thus the enhancement or reduction of inelastic flow in the matrix. Also, in conformity with the results of Brockenbrough et al. (1991) and Nakamura and Suresh (1993) a random fiber array's tensile response will be slightly greater (given a sufficiently high fiber volume content) than a hexagonal fiber arrangement. As illustrated in Fig. 7, at a 35% fiber volume fraction the hexagonal, random and square diagonal arrays all correspond. Finally, increasing the volume fraction increases the "stiffness" of the transverse tensile response of a strongly bonded system, whereas it decreases the "stiffness" in a similarly arranged yet weakly bonded system (since by increasing the volume fraction one is, in essence, increasing the number of "holes" in the matrix).

4.2 Effect of Strain Rate

Now let us examine the influence of strain rate, fiber volume fraction, and packing arrangement on the longitudinal and transverse tensile behavior given a strongly bonded system. Figure 9 illustrates the predicted longitudinal stress-strain response for two volume fractions, i.e., 35 and 50%, and the five previous fiber array geometries, given the two constant longitudinal total strain rates of 8.33×10^{-4} and 8.33×10^{-6} per second. As expected, the longitudinal tensile behavior, at a given strain rate, is independent of the packing geometry. However, significant strain rate dependence is observed, even in the longitudinal direction, due to the significant rate dependence of the matrix (TIMETAL 21S), see Fig. 10. The fact that the composite rate dependence is matrix driven is confirmed by the fact that the two order of magnitude increase in strain rate gives rise to approximately a 12% difference in stress or strain level for a 35% volume fraction whereas for a 50% volume fraction only a 7% difference is observed. This longitudinal time dependence is an important feature to remember and has largely been overlooked in the literature due to the use of time independent plasticity and/or steady state creep constitutive models. With MAC/GMC however, the use of sophisticated unified viscoplastic constituent constitutive models is computationally affordable and straightforward.

Figure 11 and 12 show, respectively, the 35 and 50 percent volume fraction transverse stress-strain tensile response, given the five different packing arrays shown in Fig. 5, which are all subjected to two constant transverse total strain rates of 8.33×10^{-4} and 8.33×10^{-6} per second. Comparing Figs. 11 and 12, one observes that: 1) the packing geometry, for a given applied strain rate, has an influence on the transverse response, 2)

increasing the strain rate or the volume fraction results in a slight increase in the packing geometry influence, and 3) the transverse composite rate dependence is greater than the neat matrix rate dependence (see Fig. 10) and this composite rate dependence slightly increases with an increase in volume fraction.

4.3 Creep Behavior

Another classic loading situation which accentuates the time dependence of the various constituents within a composite structure is that of creep. In Fig. 13 we illustrate the influence of fiber volume fraction and packing geometry on the longitudinal stress-strain and inelastic strain versus time response of SCS-6/TIMETAL 21S. Once again, as expected, the longitudinal creep response is independent of fiber packing; however, note that significant longitudinal primary creep behavior and no steady-state creep behavior are observed. This apparent transient composite creep behavior, in reality, is a result of the matrix stress being shed to the fiber and is entirely dependent on the matrix relaxation behavior. This load shedding mechanism is illustrated in Fig. 14, where the stress versus time response of the fiber, composite, and matrix are shown. Note that increasing the fiber volume fraction (e.g., from 35 to 50%) decreases the maximum stress state in the matrix (i.e., from 345 to 276 MPa) and consequently the rate of matrix relaxation (see Arnold et al. (1994a,b)). Consequently, the accumulation of the apparent longitudinal creep strain of the composite is similarly decreased. Clearly, because of this load shedding mechanism, in order to accurately predict longitudinal time dependent response (i.e., strain rate dependence or "creep" behavior) the inelastic constitutive model for the matrix must be capable of accurately predicting the matrix relaxation behavior. This fact, along with the fact that the in situ stress state in the matrix is multiaxial and nonproportional, make the use of a **GVIPS** class of unified viscoplastic model extremely attractive , see Arnold et al. (1995).

The influence of fiber packing and bond strength on the transverse creep response is now examined. Figure 15 depicts the transverse stress- strain response given the five different fiber array geometries studies previously, whereas Fig. 16 shows the strongly bonded, transverse creep strain[2] versus creep time response for the five architectures given a constant applied stress of 138 MPa. Similarly, Fig. 17 shows the transverse creep strain versus creep time response for a weakly bonded square and square diagonal fiber array geometry. Evidently, transverse creep is significant in this composite system and highly dependent upon the creep behavior of the matrix. Furthermore fiber packing and bond strength play important roles, in that the square diagonal array is the least creep resistant geometry (be it strongly or weakly bonded) whereas the square and rectangular (with low R ratio) arrays are the most creep resistant. Note, the significant increase in the creep response (as well as the "softer" tensile response) in the presence of a weakly bonded interface. For example, comparing Figs. 16 and 17, we see that the weakly bonded system accumulates approximately the same amount of inelastic strain as the

[2]Creep strain is defined as the inelastic strain incurred during a period of constant load.

strongly bonded system, but in approximately $1/36^{th}$ the time. Thus one can conclude that a weakly bonded system produces significantly higher inelastic strain rates in the matrix, due to the opening up of the fiber/matrix interfaces.

4.4 Hybrid Architecture

Although significant longitudinal specific strengths and stiffnesses are achievable in a SCS-6 reinforced TMC compared to monolithic superalloys, typically the transverse behavior is significantly less than that of the neat matrix (or superalloy) behavior due to the presence of the weak fiber/matrix interface. This disadvantage is particularly important in rotating type applications (e.g., TMC ring or impeller components) where high tensile radial stresses are present. **MAC/GMC** is ideally suited for analyzing multi-phased composites with arbitrary architecture, consequently here we will examine the influence of a hybrid (both in fiber size and bond strength) architecture on the transverse inelastic response in an attempt to mitigate this disadvantage. The proposed architecture examined consisted of a TIMETAL 21S matrix reinforced with a 35% fiber volume fraction (V_{f1}) of the larger (weakly bonded) SCS-6 fibers arranged in a square array, supplemented with a lower volume fraction (i.e., V_{f2} = 2.8, 8.75, and 17.5%) of smaller (strongly bonded) fibers, for example Al_2O_3, W, or Mo, arranged in a rectangular array, see Fig. 18. The resulting transverse stress-strain and creep strain versus creep time responses of the hybrid composite are given in Figs. 19 and 20 respectively. Clearly, both the transverse tensile and creep behavior are improved with the addition of a small fraction of strongly bonded fibers. with respect to the two-phased, weakly bonded, SCS-6/TIMETAL 21S system alone. Examining the results of the constant strain rate ($\dot{e}$ = $8.33x10^{-4}$ per second) tensile tests shown in Fig. 19, it is apparent that all three hybrid architectures analyzed still give an overall "softer" response compared to that of the monolithic matrix. However, at higher volume fractions of the smaller (strongly bonded) fibers, the initial tensile response of the hybrid composite remains "stiffer" than that of the matrix only — for over double the stress range of the two-phased system's initial response. This indicates that the presence of the smaller (strongly bonded) fibers not only adds to the transverse resistance but also reduces the extent to which the larger (weakly bonded) fiber/matrix interface opens. The creep response at an applied stress of 69 MPa, see Fig. 20, is similarly influenced by the presence of a small volume fraction (i.e., VF_2 = 17.5%) of smaller strongly bonded fibers; the creep resistance is increased three fold over that of the two-phased composite system response. Consequently, based on these results one might expect that significant improvements in the burst strength and fatigue life of TMC rings and impellers may be achieved through the use of such hybrid architectures. Note that depending upon the density of the smaller fibers, the overall weight of the system may or may not be appreciably increased. Also, the longitudinal strength of such systems may be adversely influenced if premature failure in the longitudinal directions of the smaller diameter fibers is observed. An experimental investigation into the influence

of fiber architecture including the above hybrid microstructure, is currently in progress for a SCS-6/Ti-6-4 TMC system.

4.5 Fiber Shape

Finally, it has been documented in the literature that fiber shape plays an important role in the deformation response of composites (e.g., see Adams and Donner, 1967a, or Brockenbrough et al., 1991). Here we examine three fiber shapes to verify the qualitative predictive behavior of MAC/GMC and illustrate the influence of fiber shape on the inelastic response of TMCs. The shapes studied are a square, circular and cross shaped fiber cross sections. The fiber/matrix interface is taken to be strongly bonded and the three RVEs analyzed are depicted in Fig. 21. The stress-strain responses resulting from a transverse tensile test performed at a constant strain rate of 8.33×10^{-4} per second are shown in Fig. 22; whereas the creep strain versus creep time responses resulting from an applied transverse stress of 138 MPa are shown in Fig. 23. Note, in all cases the fiber volume ratio is 35 percent and the fiber packing arrangement is square. The four tensile responses in Fig. 22 indicate that fiber shape has only a minor influence on the apparent elastic stiffness, whereas the inelastic (nonlinear) portion of the tensile response is more significantly influenced. The square fiber provides the highest triaxial (hydrostatic) state of stress within the matrix and consequently the "stiffest" (or more elastic) response, followed by the cross-shaped fiber (i.e., d=0.05 and 0.2) and then the circular shaped fiber. As one might expect, this ordering is transferred to the transverse creep response as well. The circular shaped fiber provides the least creep resistant architecture and the square fiber the most creep resistance; a two-fold increase in creep resistance relative to the circular cross section. Note that the secondary creep behavior is more dramatically influenced by fiber shape than the primary creep behavior. Also, it is important to observe that although the applied creep stress is well within the linear portion of the stress-strain response (i.e., the apparent elastic zone, see Fig. 22) significant transverse creep behavior is predicted.

5 SUMMARY/CONCLUSIONS

In summary, this three part paper has focused on the influence of fiber architecture (i.e., shape and distribution) relative to the elastic and inelastic response of metal matrix composites. The first part provided a comprehensive annotative review of the literature from a historical perspective, dealing with the effects of fiber shape and distribution on the response of continuously reinforced advanced polymeric matrix and metal matrix composites. Previous investigations dealing with both continuously and discontinuously reinforced composites were included. The second part outlined a recently developed analytical micromechanics analysis code (MAC) that is particularly well suited for studying the influence of these effects on the response of metal matrix composites. In particular, MAC/GMC is sufficiently general to predict the inelastic response of unidirectional

multi-phased composites reinforced by either continuous or discontinuous fibers with different inclusion shapes and spatial arrangements in the presence of either perfect or imperfect interfaces and/or interfacial layers.

Finally, the third part provided qualitative results generated using (MAC) for a representative titanium matrix composite system, i.e., SCS-6/TIMETAL 21S. Results were presented that correctly demonstrated (i.e., consistent with the literature) the relative effects of fiber arrangement and shape on the longitudinal and transverse stress-strain and creep response, in the presence of either strong or weak fiber/matrix interfacial bonds. The fiber arrangements included square, square diagonal, hexagonal and rectangular periodic arrays, as well as a random array. The fiber shapes included circular, square and cross-shaped cross sections. The effect of fiber volume fraction on the observed stress-strain response was included, as was the thus-far poorly documented strain rate sensitivity effect. In addition to the well documented features of architecture dependent response of continuously reinforced two-phase MMCs, new results involving continuous multi-phased internal architectures were presented. Specifically, the stress-strain and creep response of composites with different sized fibers having different internal arrangements and bond strengths was investigated with the aim of determining the feasibility of using such an approach to enhance the transverse toughness and creep resistance of TMC rings and impellers.

We now list the major conclusions drawn from this study, relative to continuous-reinforced metal matrix composites:

- MAC/GMC results are consistent with results documented in the literature regarding the relative effects of fiber arrangement and shape on the longitudinal and transverse inelastic, time dependent, response, in the presence of either strong or weak bond strengths.

- Transverse inelastic behavior is greatly influenced by fiber packing, volume fraction, bond strength and fiber shape.

- Given a rate-sensitive constituent material, the composite behavior will possess significant rate sensitivity, both longitudinally and transverse to the fiber direction; where the extent of this sensitivity is dependent upon both the fiber volume fraction and constituent property mismatch.

- Transverse toughness and creep resistance can be enhanced (relative to the standard two-phased, weakly bonded, systems) using the concept of hybrid (multiphased) architectures. The specific example hybrid architecture investigated here consisted of two different fiber diameters and bond strengths (one weak and one strong).

- The availability of MAC now provides the composites community with a comprehensive, *computationally efficient*, user-friendly, micromechanics analysis tool that:

1) admits *physically based* viscoplastic deformation and life models for each constituent of a multiphased material and 2) can analyze continuous or discontinuous multi-phased composites.

Future work will address: 1) the influence of continuous fiber architecture in the presence of residual stresses arising from processing; 2) experimentally verify the above-documented impact of fiber architecture on the inelastic behavior of an SCS-6/Ti-6-4 composite system (particularly in the case of the proposed hybrid architecture); 3) link optimization algorithms with **GMC** so as to determine the optimum architecture for a given loading history; 4) examine the influence of fiber architecture on the deformation and failure of structural components such as MMC rings, and 5) investigate the influence of discontinuous fiber architectures on inelastic behavior.

References

[1] Abel, C. A., Weissenbek, E. and Rammerstorfer, F. G. (1993), "Influence of Damage on the Mechanical Behavior of Short Fiber Reinforced MMCs with Strong and Weak Interfaces," ZAMM, Vol. 73 (4-5), T423-T426.

[2] Aboudi, J. (1988), "Constitutive Equations for Elastoplastic Composites With Imperfect Bonding", Int. Jnl. of Plasticity, Vol. 4, pp. 103-125.

[3] Aboudi, J. (1989), "Micromechanical Analysis of Composites by the Method of Cells," Applied Mechanics Reviews, Vol. 42, pp. 193-221.

[4] Aboudi, J. (1991), Mechanics of Composite Materials: A Unified Micromechanical Approach, Elsevier, The Netherlands.

[5] Aboudi, J. (1993), "Constitutive Behavior of Multiphase Metal Matrix Composites With Interfacial Damage by The Generalized Cells Model", Damage in Composite Materials, Ed., G. Z. Voyiadjis, Studies in Applied Mechanics 34, Elsevier.

[6] Aboudi, J. (1994), "Micromechanical Analysis of Thermo-Inelastic Multiphase Short-Fiber Composites," NASA CR 195290, NASA-Lewis Research Center, Cleveland, OH.

[7] Aboudi, J. and Pindera, M-J. (1992), "Micromechanics of Metal Matrix Composites Using the Generalized Method of Cells Model: User's Guide," NASA CR 190756, NASA-Lewis Research Center, Cleveland, OH.

[8] Aboudi, J., Pindera, M-J., and Arnold, S. M. (1993), "Thermoelastic Response of Metal Matrix Composites with Large-Diameter Fibers Subjected to Thermal Gradients," NASA TM 106301, NASA-Lewis Research Center, Cleveland, OH.

[9] Aboudi, J., Arnold, S. M., and Pindera, M-J. (1994a), "Response of Functionally Graded Composites to Thermal Gradients," Composites Engineering, Vol. 4, pp. 1-18.

[10] Aboudi, J., Pindera, M-J., and Arnold, S. M. (1994b), "Elastic Response of Metal Matrix Composites with Tailored Microstructures to Thermal Gradients," Int. J. Solids Structures, Vol. 31, No. 10, pp. 1393-1428.

[11] Aboudi, J., Pindera, M-J., and Arnold, S. M. (1995), "Thermo-Inelastic Response of Functionally Graded Composites," Int. J. Solids and Structures, Vol. 32, No. 12, pp. 1675-1710.

[12] Adams, D. F. and Doner, D. R. (1967a), "Longitudinal Shear Loading of a Unidirectional Composite," J. Composite Materials, Vol. 1, pp. 4-17.

[13] Adams, D. F. and Doner, D. R. (1967b), "Transverse Normal Loading of a Unidirectional Composite," J. Composite Materials, Vol. 1, pp. 152-164.

[14] Adams, D. F. and Tsai, S. W. (1969), "The Influence of Random Filament Packing on the Transverse Stiffness of Unidirectional Composites," J. Composite Materials, Vol. 3, pp. 368-381.

[15] Adams, D. F. (1970), "Inelastic Analysis of a Unidirectional Composite Subjected to Transverse Normal Loading," J. Composite Materials, Vol. 4, pp. 310-328.

[16] Arnold, S.M.; Wilt, T.E., Saleeb, A.F., and Castelli, M.G. (1993), "An Investigation of Marco and Micromechanical Approaches for a Model MMC System", HITEMP Review 1993, NASA CP 19117, pp. 52:1-12.

[17] Arnold, S.M.; and Saleeb, A.F., (1994), "On the Thermodynamic Framework of Generalized Coupled Thermoelastic Viscoplastic - Damage Modeling", Int. Jnl. of Plasticity, Vol. 10, No. 3, pp. 263-278, Also NASA TM 105349, 1991.

[18] Arnold, S.M.; Saleeb, A.F., and Castelli, M.G., (1994a), "A Fully Associative, Nonlinear Kinematic, Unified Viscoplastic Model for Titanium Based Matrices", NASA TM-106609.

[19] Arnold, S.M.; Saleeb, A.F., and Castelli, M.G., (1994b) "A Fully Associative, Nonisothermal, Nonlinear Kinematic, Unified Viscoplastic Model for Titanium Alloys", NASA TM-106926.

[20] Arnold, S.M., Saleeb, A.F., and Wilt, T.E. (1995), A Modeling Investigation of Thermal and Strain Induced Recovery and Nonlinear Hardening in Potential Based Viscoplasticity, Jnl. of Engng. Mat. and Tech., Vol. 117, No. 2, pp.157-167. Also NASA TM-106122, 1993.

[21] Ashton, J. E., Halpin, J. C. and Petit, P. H. (1969), Primer on Composite Materials: Analysis, pp. 77-81, Technomic Publishing Co., Stamford, Conn.

[22] Bao, G., Hutchinson, J. W. and McMeeking, R. M. (1991), "Particle Reinforcement of Ductile Matrices Against Plastic Flow and Creep," Acta metall. metar., Vol. 39, No. 5, pp. 1871-1882.

[23] Bigelow, C. A. (1992), "The Effects of Uneven Fiber Spacing on Thermal Residual Stresses in a Unidirectional SCS-6/Ti-15-3 Laminate," J. Composites Technology

[24] Bohm, H. J., Rammerstorfer, F. G. and Weissenbek, E. (1993), "Some Simple Models for Micromechanical Investigations of Fiber Arrangement Effects in MMCs," Computational Materials Science, Vol. 1, pp. 177-194.

[25] Brockenbrough, J. R. and Suresh, S. (1990), "Plastic Deformation of Continuous Fiber-Reinforced Metal-Matrix Composites: Effects of Fiber Shape and Distribution," Scripta Metallurgica and Materialia, Vol. 24, pp. 325-330.

[26] Brockenbrough, J. R., Suresh, S. and Wienecke, H. A. (1991), "Deformation of Metal-Matrix Composites with Continuous Fibers: Geometrical Effects of Fiber Distribution and Shape," Acta metall. metar., Vol. 39, No. 5, pp. 735-752.

[27] Brown, L. M. and Clarke, D. R. (1975), "Work Hardening Due to Internal Stresses in Composite Materials," Acta Metall., Vol. 23, pp. 821-830.

[28] Chamis, C. C. and Sendeckyj, G. P. (1968), "Critique on Theories Predicting Thermoelastic Properties of Fibrous Composites," J. Composite Materials, Vol. 2, No. 3, pp. 332-358.

[29] Christman, T., Needleman, A. and Suresh, S. (1989), "An Experimental and Numerical Study of Deformation in Metal-Ceramic Composites," Acta metall. mater., Vol. 37, No. 11, pp. 3029-3050.

[30] Crossman, F. W., Karlak, R. F. and Barnett, D. M. (1974), "Creep of B/Al Composites as Influenced by Residual Stress, Bond Strength, and Fiber Packing Geometry," in Failure Modes in Composites II, pp. 8-31, TMS of AIME Publication, New York.

[31] Crossman, F. W. and Karlak, R. F. (1976), "Multiaxial Creep of Metal Matrix Fiber Reinforced Composites," in Failure Modes in Composites III, pp. 260-287, T. T. Chiao and D. M. Schuster, Eds. TMS of AIME Publication (Proc. 105th AIME Annual Meeting).

[32] Dow, N. F. (1963), General Electric Report No. R63-SD61.

[33] Dragone, T. L. and Nix, W. D. (1990), "Geometric Factors Affecting the Internal Stress Distribution and High Temperature Creep Rate of Discontinuous Fiber Reinforced Metals," Acta metall. mater., Vol. 38, No. 10, pp. 1941-1953.

[34] Drucker, D. C. (1965), "Engineering and Continuum Aspects of High-Strength Materials," in High-Strength Materials, V. F. Zackay, Ed., pp. 795-833, John Wiley and Sons, Inc.

[35] Dvorak, G. J., Rao, M. S. M. and Tarn, J. Q. (1973), "Yielding in Unidirectional Composites Under External Loads and Temperature Changes," J. Composite Materials, Vol. 7, pp. 194-216.

[36] Dvorak, G. J., Rao, M. S. M. and Tarn, J. Q. (1974), "Generalized Initial Yield Surfaces for Unidirectional Composites," J. Applied Mechanics, Vol. 41, pp. 249-253.

[37] Eshelby, D. (1957), "The Determination of the Elastic Field of an Ellipsoidal Inclusion, and Related Problems, " Proc. Royal Soc. (London), Vol. A 241, pp. 376-396.

[38] Foye, R. L. (1966a), "An Evaluation of Various Engineering Estimates of the Transverse Properties of Unidirectional Composites," SAMPE, Vol. 10, pp. G31-G42.

[39] Foye, R. L. (1966b), "Structural Composites," Quarterly Progress Reports No. 1 and 2, AFML Contract No. AF33(615)-5150.

[40] Foye, R. L. (1973), "Theoretical Post-Yielding Behavior of Composite Laminates. Part I - Inelastic Micromechanics," J. Composite Materials, Vol. 7, pp. 178-193.

[41] Ghosh, S. and Moorthy, S. (1995), "Elastic-Plastic Analysis of Arbitrary Heterogeneous Materials with the Voronoi Cell Finite Element Method", Comput. Methods Appl. Mech. Engrg. Vol. 121, pp. 373-409.

[42] Ghosh, S., Lee, K. and Moorthy, S. (1995), "Multiple Scale Analysis of Heterogeneous Elastic Structures Using Homogenization Theory and Voronoi Cell Finite Element Method", Int. J. Solids Structures, Vol. 32, No. 1, pp. 27-62.

[43] Halpin, J. C. and Tsai, S. W. (1967), "Environmental Factors in Composite Materials Design," AFML TR 67-423.

[44] Hashin, Z. and Shtrikman, S. (1963), "A Variational Approach to the Theory of the Elastic Behavior of Multiphase Media," J. Mech. Phys. Solids, Vol. 11, pp. 127-140.

[45] Hashin, Z. and Rosen, B. W. (1964), "The Elastic Moduli of Fiber-Reinforced Materials," J. Applied Mechanics, Vol. 31, pp. 223-232.

[46] Hashin, Z. (1965), "On Elastic Behavior of Fibre Reinforced Materials of Arbitrary Transverse Phase Geometry," J. Mech. Phys. Solids, Vol. 13, pp. 119-134.

[47] Hashin, Z. (1972), "Theory of Fiber Reinforced Materials," NASA CR-1974, NASA-Langley Research Center, Hampton, VA.

[48] Hermans, J. J. (1967), "The Elastic Properties of Fiber Reinforced Materials when the Fibers are Aligned," Proc. Konigl. Nederl. Akad. van Weteschappen Amsterdam, Vol. B70(1), p. 1.

[49] Hill, R. (1965), "A Self-Consistent Mechanics of Composite Materials," J. Mech. Phys. Solids, Vol. 13, pp. 213-222.

[50] Hulbert, L. E. and Rybicki, E. F. (1971), "Boundary Point Least Squares Analysis of the Free Edge Effects in Some Unidirectional Fiber Composites," J. Composites Materials, Vol. 5, pp. 164-175.

[51] Johnson, W. S., Lubowinski, S. J., and Highsmith, A. L. (1990), "Mechanical Characterization of Unnotched SCS6/Ti-15-3 Metal Matrix Composites at Room Temperature," In ASTM STP 1080 (edited by J. M. Kennedy, H.H. Moeller and W. S. Johnson), pp. 193-218. American Society for Testing and Materials, Philadelphia, PA.

[52] Karbhari, V. M. and Wilkins, D. J. (1991), "Constituent Scale and Property Effects on Fibre-Matrix Debonding and Pull-Out," J. Materials Science, Vol. 26, pp. 5888-5898.

[53] Karlak, R. F., Crossman, F. W. and Grant, J. J. (1974), "Interface Failures in Composites," in Failure Modes in Composites II, pp. 119-130, TMS of AIME Publication, New York.

[54] Karlak, R. F. and Crossman, F. W. (1976), "Theoretical Off-Axis Response of Idealized Composites," in Failure Modes in Composites III, pp. 288-301, T. T. Chiao and D. M. Schuster, Eds. TMS of AIME Publication (Proc. 105th AIME Annual Meeting).

[55] Kolle, J. J. and Mueller, A. C. (1991), "Automated Modeling of Composite Physical Properties (U)," Quest Integrated Technical Report No. 533, Quest Integrated, Inc., Kent, Washington 98032.

[56] Komenda, J. and Henderson, P. J. (1993), "Quantification of Fibre Distribution in a Metal Matrix Composite and its Effect on Creep Rupture Properties," Scripta Metallurgica and Materialia, Vol. 28, pp. 553-558.

[57] Leissa, A. W. and Clausen, W. E., (1968), "Application of Point Matching to Problems in Micromechanics," in Fundamental Aspects of Fiber Reinforced Plastic Composites, pp. 29-44, R. T. Schwartz and H. S. Schwartz, Eds. Interscience Publishers, New York.

[58] Lerch B.A. and Saltsman, J.F. (1993), "Tensile Deformation of SiC/Ti-15-3 Laminates", Composite Materials: Fatigue and Fracture, Fourth Volume, ASTM STP 1156, W. W. Stinchcomb and N.E.Ashbaugh, Eds., ASTM, pp. 161 -175.

[59] Levy, A. and Papazian, J. M. (1990), "Tensile Properties of Short Fiber-Reinforced SiC/Al Composites: Part II. Finite-Element Analysis," Metall. Trans. A, Vol. 21A, pp. 411-420.

[60] Lin, T. H., Salinas, D. and Ito, Y. M. (1972a), "Initial Yield Surface of a Unidirectionally Reinforced Composite," J. Applied Mechanics, Vol. 39, pp. 321-326.

[61] Lin, T. H., Salinas, D. and Ito, Y. M. (1972b), "Elastic-Plastic Analysis of Unidirectional Composites," J. Composite Materials, Vol. 6, pp. 48-60.

[62] Lissenden, C. J., Pindera, M-J., and Herakovich, C. T. (1994), "Stiffness Degradation of SiC/Ti Tubes Subjected to Biaxial Loading,"Composites Science and Technology, Vol. 50, pp. 23-36.

[63] Lu, T. C., Yang, J., Suo, Z., Evans, A. G., Hecht, R. and Mehrabian, R. (1991), "Matrix Cracking in Intermetallic Composites Caused by Thermal Expansion Mismatch," Acta metall. mater., Vol. 39, No. 8, pp. 1883-1890.

[64] MacKay, R. A. (1990), "Effect of Fiber Spacing on Interfacial Damage in a Metal Matrix Composite," Scripta Metallurgica et Materialia, Vol. 24, pp. 167-172.

[65] Majumdar, B. S. and Newaz, G. M. (1992), "Inelastic Deformation of Metal Matrix Composites: Plasticity and Damage Mechanisms," Philosophical Magazine, Vol. 66, No. 2, pp. 187-212.

[66] McHugh, P. E., Asaro, R. J. and Shih, C. F. (1993a), "Computational Modeling of Metal Matrix Composite Materials - I. Isothermal Deformation Patterns in Ideal Microstructures," Acta metall. mater., Vol. 41, No. 5, pp. 1461-1476.

[67] McHugh, P. E., Asaro, R. J. and Shih, C. F. (1993b), "Computational Modeling of Metal Matrix Composite Materials - II. Isothermal Stress-Strain Behavior," Acta metall. mater., Vol. 41, No. 5, pp. 1477-1488.

[68] McHugh, P. E., Asaro, R. J. and Shih, C. F. (1993c), "Computational Modeling of Metal Matrix Composite Materials - III. Comparisons with Phenomenological Models," Acta metall. mater., Vol. 41, No. 5, pp. 1489-1499.

[69] McHugh, P. E., Asaro, R. J. and Shih, C. F. (1993d), "Computational Modeling of Metal Matrix Composite Materials - VI. Thermal Deformations," Acta metall. mater., Vol. 41, No. 5, pp. 1501-1510.

[70] Mori, T. and Tanaka, K. (1973), "Average Stress in Matrix and Average Energy of Materials with Misfitting Inclusions," Acta Metall., Vol. 21, pp. 571-574.

[71] Mueller, A. C. (1994), "A Finite Element Method for Microstructural Analysis" Composites Engineering, Vol. 4, No. 3, pp. 361-376.

[72] Nakamura, T. and Suresh, S. (1993), "Effects of Thermal Residual Stresses and Fiber Packing on Deformation of Metal-Matrix Composites," Acta metall. mater., Vol. 41, No. 6, pp. 1665-1681.

[73] Nemat-Nasser, S. and Iwakuma, T. (1982), "On Composites with Periodic Structures," Mechanics of Materials, Vol. 1, pp. 239-267.

[74] Nemat-Nasser, S. and Hori, M. (1993), Micromechanics: Overall Properties of Heterogeneous Materials, North-Holland, New York.

[75] Nimmer, R. P., Bankert, R. J., Russell, E. S., Smith, G. A. and Wright, P. K. (1991a), "Micromechanical Modeling of Fiber/Matrix Interface Effects in Transversely Loaded SiC/Ti-6-4 Metal Matrix Composites," J. Composites Technology

[76] Nimmer, R. P., Siemers, P. A. and Eggleston, M. R. (1991b), "Fiber Array Geometry Effects Upon Composite Transverse Tensile Behavior," Titanium Aluminide Composites, WL-TR-91-4020, P. R. Smith, S. J. Balsone and T. Nicholas, Eds. pp. 596-619.

[77] Ochiai, S. and Osamura, K (1989a), "Stress Disturbance Due to Broken Fibres in Metal Matrix Composites with Non-Uniform Fibre Spacing," J. Materials Science, Vol. 24, pp. 3865-3872.

[78] Ochiai, S. and Osamura, K (1989b), "Tensile Strength of Fibre-Reinforced Metal Matrix Composites with Non-Uniform Fibre Spacing," J. Materials Science, Vol. 24, pp. 3536-3540.

[79] Pagano, N.J. and Brown, H. W. (1993), "The Full-Cell Cracking Mode in Unidirectional Brittle - Matrix Composites, " Composites, Vol. 24, No. 2, pp. 69-83.

[80] Paley, M. and Aboudi, J. (1992), "Micromechanical Analysis of Composites by the Generalized Cells Model," Mechanics of Materials, Vol. 14, pp. 127-139.

[81] Papazian, J. M. and Adler, P. N. (1990), "Tensile Properties of Short Fiber-Reinforced SiC/Al Composites: Part I. Effects of Matrix Precipitates," Metall. Trans. A, Vol. 21A, pp. 401-410.

[82] Pickett, G. (1968), "Elastic Moduli of Fiber Reinforced Plastic Composites," in Fundamental Aspects of Fiber Reinforced Plastic Composites, pp. 13-27, R. T. Schwartz and H. S. Schwartz, Eds. Interscience Publishers, New York.

[83] Pindera, M-J. (1993), "Micromechanical Aspects of Yielding and Failure Criteria of Composites," in Failure Criteria of Structured Media (Proc. CNRS Int. Colloquium No. 351, 1983), pp. 121-143, J. P. Boehler, Ed., A. Balkema, Rotterdam.

[84] Povirk, G. L., Needleman, A. and Nutt, S. R. (1990), "An Analysis of Residual Stress Formation in Whisker-Reinforced Al-SiC Composites," Materials Science and Engineering, Vol. A125, pp. 129-140.

[85] Povirk, G. L. et al. (1992), "Thermally and Mechanically Induced Residual Stresses in Al-SiC Composites," Acta metall. mater., Vol. 40, No. 9, pp. 2391-2412.

[86] Robertson, D.D. and Mall, S. (1993), "Micromechanical Relations for Fiber-Reinforced Composites Using the Free Transverse Shear Approach", JCTRER, Vol. 15, No. 3, pp. 181-192.

[87] Robertson, D.D. and Mall, S. (1994), "Micromechanical Analysis of Metal Matrix Composite Laminates With Fiber/Matrix Interfacial Damage", Composites Engineering, Vol. 4, No. 2, pp. 1257-1274.

[88] Shen, Y.-L., Finot, M., Needleman, A. and Suresh, S. (1994), "Effective Elastic Response of Two-Phase Composites," Acta metall. mater., Vol. 42, No. 1, pp. 77-97.

[89] Siegmund, Th., Weissenbek, E., Fischer, F. D. and Rammerstorfer, F. G. (1992), "Micromechanical Consideration of Topological Aspects Regarding Thermocyclic Behavior," in The Processing, Properties and Applications of Metallic and Ceramic Materials, Vol. II, MCE, pp. 971-976, M. H. Loretto and C. J. Beevers, Eds., Birmingham, U.K.

[90] Tvergaard, V. (1990), "Analysis of Tensile Properties for a Whisker-Reinforced Metal-Matrix Composite," Acta metall. mater., Vol. 38, No. 2, pp. 185-194.

[91] Walker, K. P., Jordan, E. H., and Freed, A. D. (1989), "Nonlinear Mesomechanics of Composites with Periodic Microstructure: First Report," NASA TM 102051, NASA-Lewis Research Center, Cleveland, OH.

[92] Walker, K. P., Freed, A. D., and Jordan, E. H. (1991), "Microstress Analysis of Periodic Composites," Composites Engineering, Vol. 1, pp. 29-40.

[93] Weissenbek, E. and Rammerstorfer, F. G. (1993), "Influence of the Fiber Arrangement on the Mechanical and Thermo-Mechanical Behavior of Short Fiber Reinforced MMCs," Acta metall. mater., Vol. 41, No. 10, pp. 2833-2843.

[94] Weissenbek, E., Bohm, H. J. and Rammerstorfer, F. G. (1993), "Microgeometrical Effects on the Elastoplastic Behavior of Particle Reinforced MMCs," in ICCM/9, A. Miravete, Ed., University of Zaragoza, Woodhead Publishing Limited.

[95] Wilt, T.E. and Arnold, S.M., (1994), "Micromechanics Analysis Code (MAC) User Guide: Version 1.0", NASA TM 106706.

[96] Wilt, T.E. (1995), "On The Finite Element Implementation of the Generalized Method of Cells Micromechanics Constitutive Model", NASA CR 195451.

[97] Wisnom, M. R. (1990), "Factors Affecting the Transverse Tensile Strength of Unidirectional Continuous Silicon Carbide Fibre Reinforced 6061 Aluminum," J. Composite Materials, Vol. 24, pp. 707-726.

[98] Zhenhai, X., Zhiying, M. and Yaohe, Z. (1991), "Effect of Fibre Distribution on Infiltration Processing and Fracture Behavior of Carbon Fibre-Reinforced Aluminum Composites," Zeitschrift fur Metallkunde, Vol. 8, No. 10, pp. 766-768.

[99] Yang, J., Pickard, S. M., Cady, C., Evans, A. G. and Mehrabian, R. (1991), "The Stress-Strain Behavior of Aluminum Matrix Composites with Discontinuous Reinforcements," Acta metall. mater., Vol. 39, No. 8, pp. 1863-1869.

Table I. Summary of references providing explicit comparison of the elastic response of continuously reinforced composites with different fiber architectures.

Reference	Fiber shape and array geometry	Elastic moduli	Fiber/matrix
Hashin and Rosen (1964)	circular fibers in a hexagonal array, and circular fibers of unequal cross sections in a random array (variational elasticity treatment)	G_{12} versus v_f	Gl/Ep
Hashin (1965)	statistically homogeneous distribution of fibers with arbitrary cross-sections (variational elasticity treatment)	G_{12}, G_{23} and K_{23} (upper and lower bounds)	N/A
Foye (1966a,b)	circular fibers in square and hexagonal arrays, elliptical fibers in a hexagonal array, diamond and rectangular fibers in a diamond array (finite-element analysis of a unit cell)	ν_{12}, ν_{23}, E_{22} and G_{12} versus v_f	Gl/Ep
Adams and Donner (1967a)	circular, elliptical and square fibers with equal spacing in the transverse plane (finite-difference analysis of a unit cell)	G_{12} versus filament spacing, G_{12} at selected v_f for different G_f/G_m ratios	B/Ep, Gl/Ep, Gr/Ep
Pickett (1968)	circular fibers in rectangular and hexagonal arrays (elasticity analysis of a unit cell)	C_{ij} components for selected v_f	Gl/Ep
Adams and Tsai (1969)	circular fibers in periodic and random square and hexagonal arrays (finite-element analysis of a unit cell)	E_{22} versus v_f	Gl/Ep
Ashton et al. (1969)	circular fibers in square and hexagonal arrays, rectangular fibers in a diamond array (finite-difference and finite-element analysis of a unit cell)	E_{22}, G_{12} versus v_f (rectangular fibers with different aspect ratios), E_{22} vs v_f (circular fibers in square and hexagonal arrays)	Gl/Ep, B/Ep
Hashin (1972)	an infinite array of composite cylinders of continuously varying sizes that completely fill the composite space (variational and exact elasticity analysis of a fiber/matrix composite cylinder)	G_{12} versus v_f, E_{22} versus v_f	Gl/Ep

Table II. Summary of references providing explicit comparison of the elastic/inelastic response of continuously reinforced composites with different fiber architectures.

Reference	Fiber shape and array geometry	Elastic moduli	Inelastic response	Fiber/matrix
Adams (1970)	circular fibers in square and rectangular arrays	None given	$\sigma_{22} - \varepsilon_{22}$ (elastoplastic)	B/Al
Crossman et al. (1974)	circular fibers in square, hexagonal and diamond arrays	None given	$\dot{\varepsilon}_{22} - \sigma_{22}$ (steady-state creep)	B/Al
Crossman and Karlak (1976)	circular fibers in square, hexagonal and diamond arrays	None given	$\dot{\varepsilon}_{22} - \sigma_{22}$ (steady-state creep) $\dot{\varepsilon}_{12} - \sigma_{12}$ (steady-state creep)	B/Al
Karlak and Crossman (1976)	circular fibers in square, square-diagonal and hexagonal arrays	$E_{11}, E_{22}, G_{12}, \nu_{12}, \nu_{23}$ for selected ν_f, E_{xx} versus θ	σ_{11}^{y} for selected ν_f, $\sigma_{xx}^{y} - \theta$	B/Al
Wisnom (1990)	circular fibers in rectangular and diamond arrays	E_{22}, ν_{23}	σ_{22}^{ult} (weak interface)	SiC/Al
Nimmer et al. (1991)	circular fibers in square and rectangular arrays	None given	$\sigma_{22} - \varepsilon_{22}$ (elastoplastic, weak interface)	SiC/Ti
Brockenbrough et al. (1991)	circular and square fibers in square, square-diagonal, triangular and random arrays; hexagonal fibers in a triangular array	$E_{11}, E_{22}, G_{23}, \nu_{12}$	$\sigma_{11} - \varepsilon_{11}$ (elastoplastic) $\sigma_{22} - \varepsilon_{22}$ (elastoplastic) $\sigma_{23} - \varepsilon_{23}$ (elastoplastic)	B/Al
Nakamura and Suresh (1993)	circular fibers in square, square-diagonal, hexagonal and random arrays	$E_{11}, E_{22}, G_{23}, \alpha_{22}$	$\sigma_{11} - \varepsilon_{11}$ (elastoplastic) $\sigma_{22} - \varepsilon_{22}$ (elastoplastic) $\varepsilon_{22}^{th} - \Delta T$ (thermoplastic)	B/Al
Bohm et al. (1993)	circular fibers in square, square-diagonal, diamond and quasi-random arrays	$E_{11}, E_{22}, \nu_{12}, \alpha_{11}, \alpha_{22}$	σ_{11}^{y}, σ_{22}^{y} (initial yield stress) $\sigma_{11} - \varepsilon_{11}$ (elastoplastic) $\sigma_{22} - \varepsilon_{22}$ (elastoplastic)	B/Al
Mueller (1994)	circular fibers in square and hexagonal arrays, square fibers in a square array	$E_{11}, E_{22}, G_{12}, G_{23}, \nu_{12}, \nu_{23}, \alpha_{11}, \alpha_{22}$	$\sigma_{12} - \varepsilon_{12}$ (elastoplastic) $\sigma_{22} - \varepsilon_{22}$ (elastoplastic) $\sigma_{23} - \varepsilon_{23}$ (elastoplastic)	B/Al

Note: finite-element analysis of a unit cell model used in all of the above references.

Table III. Summary of references providing explicit comparison of the elastic/inelastic response of discontinuously reinforced composites with different fiber architectures.

Reference	Fiber shape and array geometry	Elastic moduli	Inelastic response	Fiber/matrix
Brown and Clarke (1975)	spherical and disk-like inclusions in macroscopically uniform arrays	None given	$\bar{\sigma}_m, \bar{\varepsilon}_m$	
Christman et al. (1989)	cylindrical and spherical inclusions in hexagonal, unstaggered arrays, rectangular inclusions in clustered arrays	None given	$\sigma_{11} - \varepsilon_{11}$ (elastoplastic)	Al-SiC
Tvergaard (1990)	cylindrical inclusions in hexagonal, staggered arrays	None given	$\sigma_{11} - \varepsilon_{11}$ (elastoplastic)	Al-SiC
Povirk et al. (1990)	cylindrical inclusions in hexagonal, unstaggered arrays	None given	Residual stresses for several fiber and cell aspect ratios, and fiber concentrations (thermoplastic)	Al-SiC
Papazian and Adler (1990)	as-fabricated whisker and particulate-reinforced composites	E_{11}	$\sigma_{11} - \varepsilon_{11}$ (elastoplastic)	Al-SiC
Levy and Papazian (1990)	cylindrical inclusions in square, unstaggered and staggered arrays	$E_{11}, E_{22}, \nu_{12}, \nu_{21}$	$\sigma_{11} - \varepsilon_{11}$ (elastoplastic)	Al-SiC
Dragone and Nix (1990)	cylindrical inclusions in cylindrical, unstaggered arrays, rectangular inclusions in clustered arrays	None given	ε_{11} – time (creep), $\dot{\varepsilon}_{11}$ – fiber distance, aspect ratio, overlap (creep)	Al-SiC
Bao et al. (1991)	cylindrical, spherical and ellipsoidal inclusions in hexagonal, unstaggered arrays, needle-like and disk-like inclusions in packet-like morphology	None given	σ_{11}^{flow} – aspect ratio, $\sigma_{11} - \varepsilon_{11}$ (elastoplastic)	
Povirk et al. (1992)	cylindrical, conical and ellipsoidal inclusions in hexagonal, unstaggered arrays	None given	$\sigma_{11} - \varepsilon_{11}$ (elastoplastic)	Al-SiC

Note: finite-element analysis of a unit cell model used in all of the above references.

Table III (cont'd). Summary of references providing explicit comparison of the elastic/inelastic response of discontinuously reinforced composites with different fiber architectures.

Reference	Fiber shape and array geometry	Elastic moduli	Inelastic response	Fiber/matrix
Yang et al. (1991)	as-fabricated composites reinforced with SiC particulates and randomly-oriented platelets	E_{11} versus v_f	$\sigma_{11} - \varepsilon_{11}$ (elastoplastic)	Al-SiC
Lu et al. (1991)	circular fibers in cubic and hexagonal arrays	None given	Stress intensity factor versus crack length for radial cracks at the fiber/matrix interface	
Siegmund et al. (1992)	cylindrical inclusions in hexagonal, staggered and unstaggered arrays	None given	ε_{11} – temperature (elastoplastic)	Al-$Al_2O_3SiO_2$
McHugh et al. (1993a-d)	hexagonal inclusions in periodic arrays of various morphologies	None given	$\sigma_{11} - \varepsilon_{11}$ (crystallographic viscoplastic theory)	
Abel et al. (1993)	cylindrical inclusions in hexagonal, staggered and unstaggered arrays	None given	$\sigma_{11} - \varepsilon_{11}$ (elastoplastic) $\sigma_{22} - \varepsilon_{22}$ (elastoplastic) (interfacial debonding and deformation-induced damage)	Al-$Al_2O_3SiO_2$
Weissenbek and Rammerstorfer (1993)	cylindrical inclusions in hexagonal, staggered and unstaggered arrays	None given	ε_{11} – temperature (elastoplastic) ε_{22} – temperature (elastoplastic) $\sigma_{11} - \varepsilon_{11}$ (elastoplastic with deformation-induced damage)	Al-Al_2O_3
Weissenbek et al. (1993)	cubical, cylindrical and spherical inclusions in simple, face-center body-center cubic arrays, cylindrical inclusions in hexagonal, staggered and unstaggered arrays	None given	$\sigma_{11} - \varepsilon_{11}$ (elastoplastic) ε_{11} – temperature (elastoplastic) ε_{22} – temperature (elastoplastic)	Al-SiC
Shen et al. (1994)	cylindrical, octagonal, conical and spherical inclusions in hexagonal, unstaggered arrays, different-sized square inclusions in square arrays	E versus v_f	None given	

Note: finite-element analysis of a unit cell model used in all of the above references.

CPU Time Comparisons

GMC		Finite Element					
case	CPU time	mesh size →	4	16	64	272	1088
4-cell	1.(1.17s)	CPU time	21	25	115	1130	15000
49-cell	1.(5.07s)	CPU time	5	6	27	261	3550

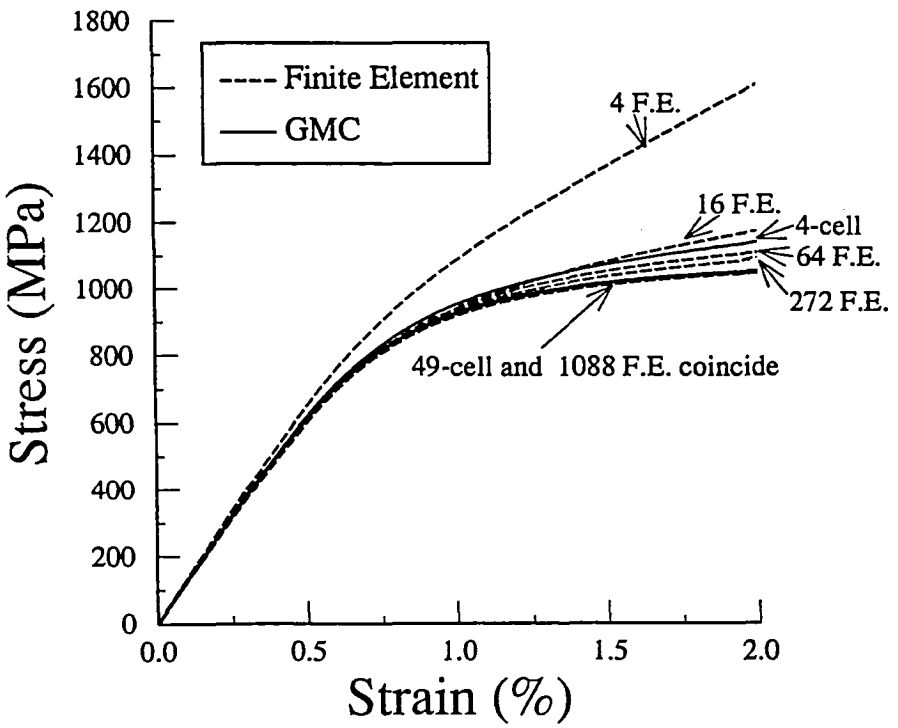

Figure 1: Comparison of the computational speed and accuracy of the generalized method of cells (GMC) to the finite element unit cell approach.

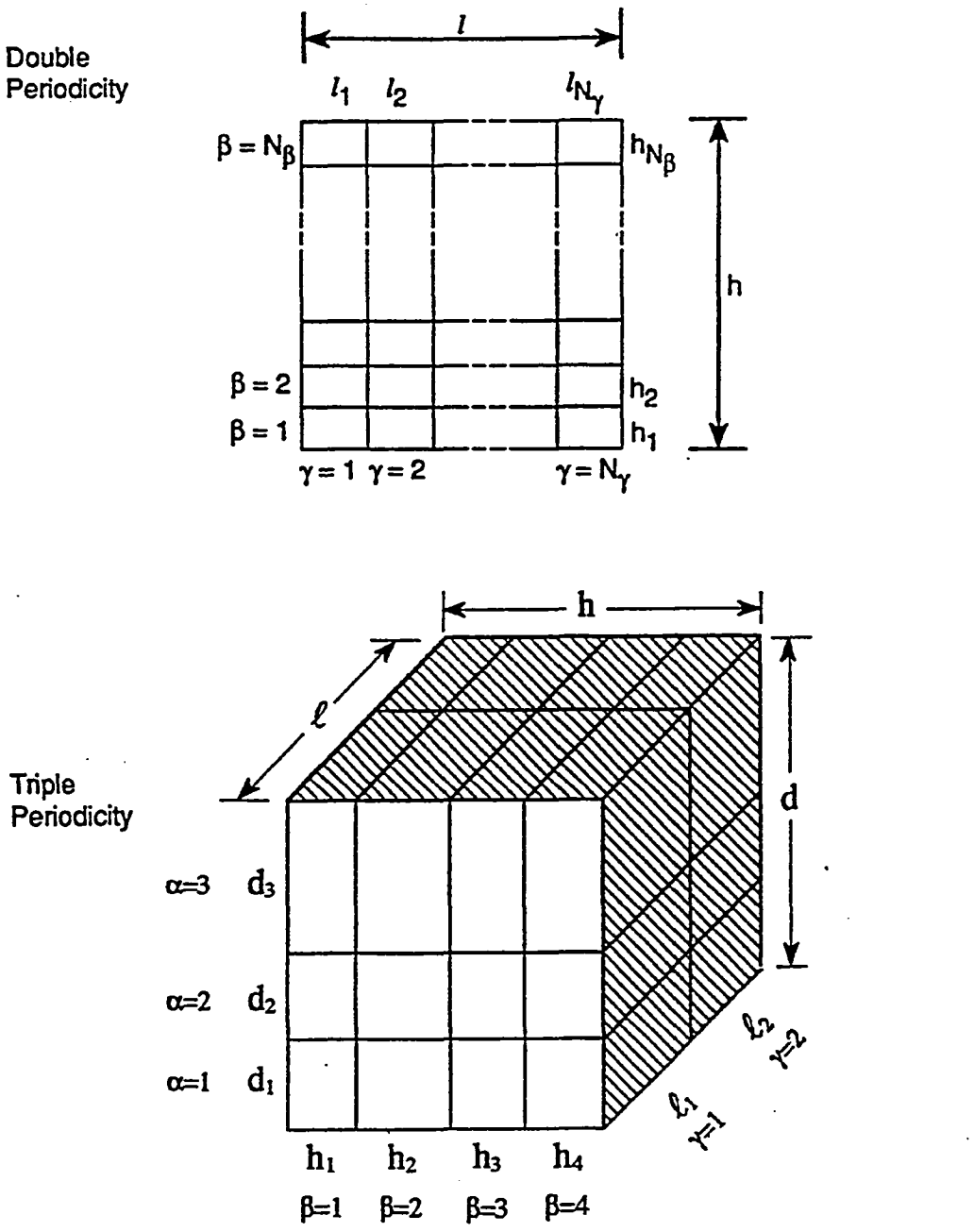

Figure 2: Generalized Method of Cells, subcell dimension nomenclature for both double and triple periodicity conditions.

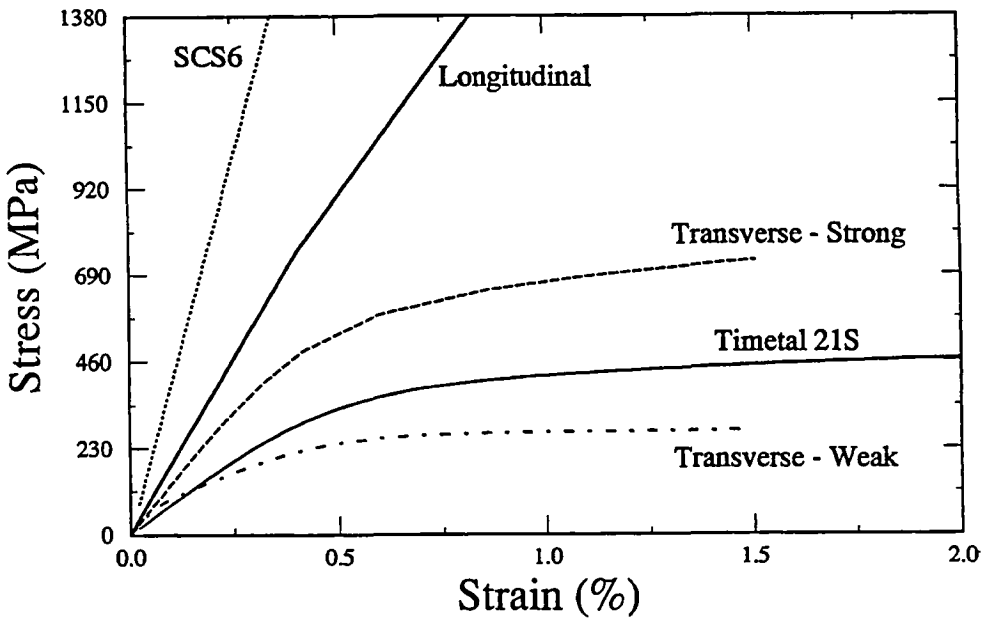

Figure 3: Qualitative tensile behavior of 35% volume fraction TMC system and its constituents given a total strain rate of 8.33×10^{-4} /sec.

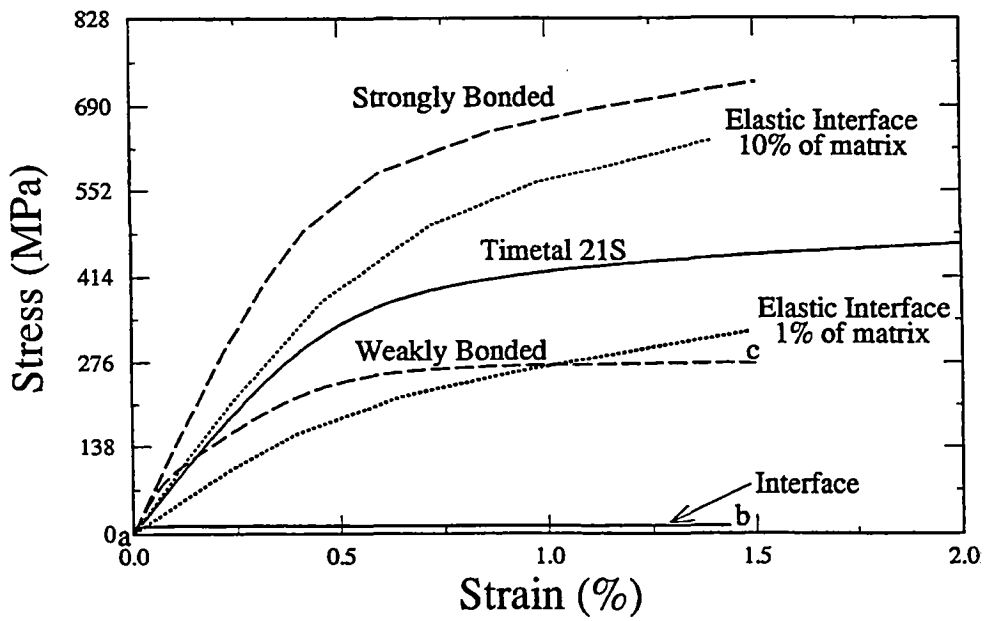

Figure 4: Qualitative transverse tensile behavior of 35% volume fraction TMC system with different interfacial consitutive models (i.e., purely elastic and elasto-perfectly-viscoplastic) to simulate a weak fiber/matrix bond.

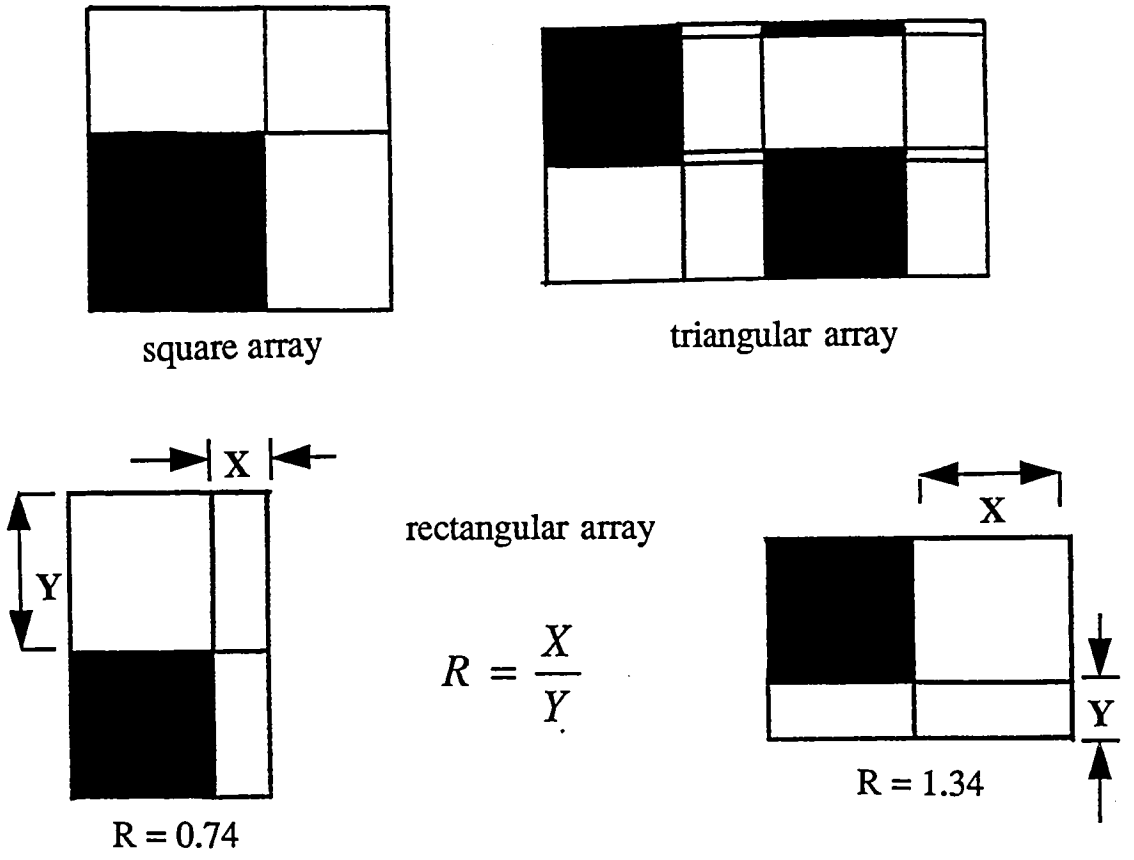

Figure 5: The representative volume elements of the five fiber packing arrays examined, i.e. square, triangular (or hexagonal), rectangular with R= 0.74 and 1.34, and square diagonal.

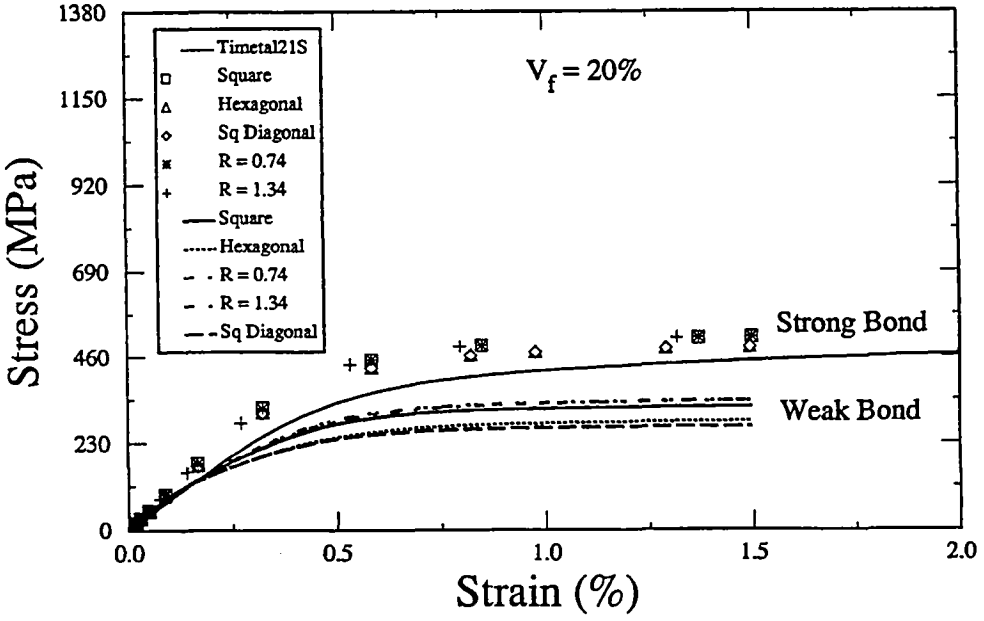

Figure 6: Influence of bond strength and packing arrangement on the transverse tensile response of 20% fiber volume fraction TMC system.

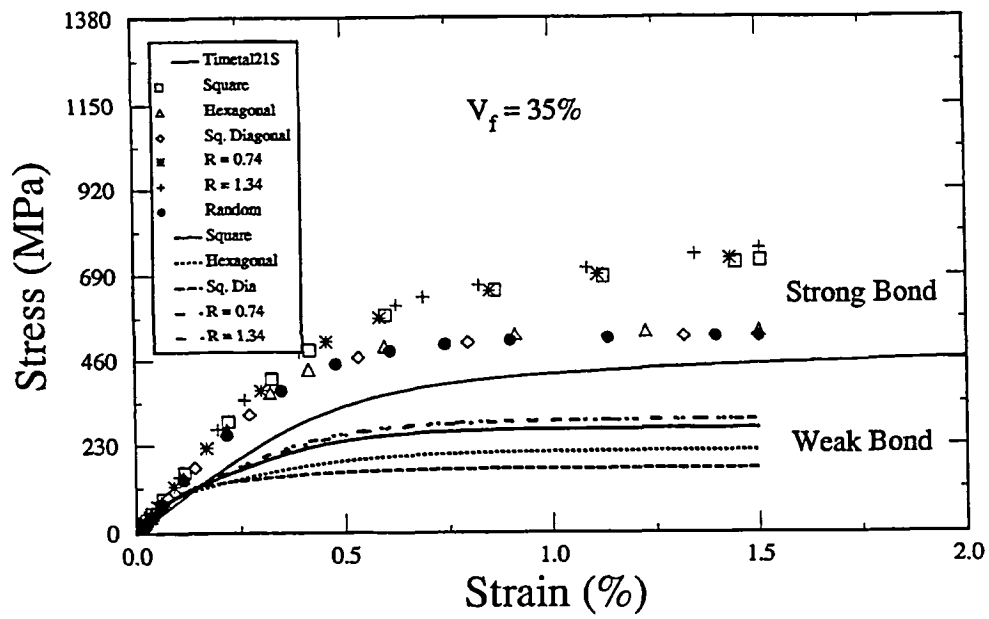

Figure 7: Influence of bond strength and packing arrangement on the transverse tensile response of 35% fiber volume fraction TMC system.

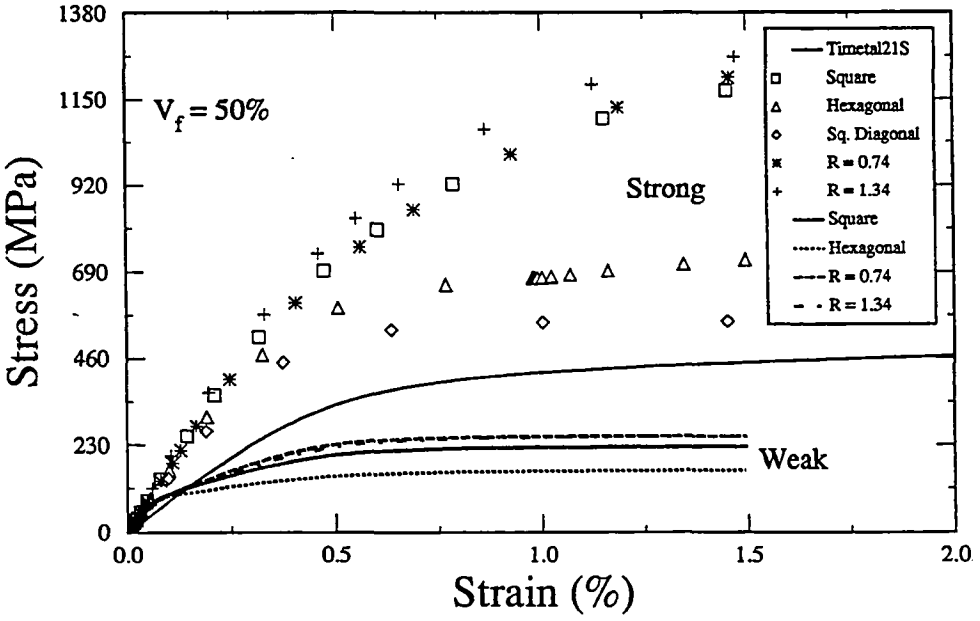

Figure 8: Influence of bond strength and packing arrangement on the transverse tensile response of 50% fiber volume fraction TMC system.

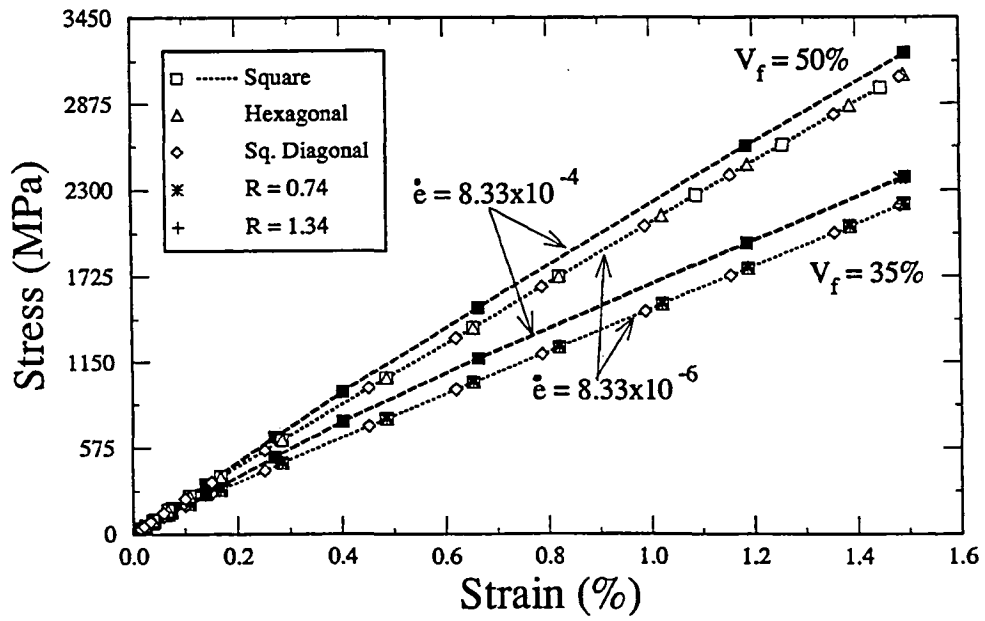

Figure 9: Influence of strain rate, volume fraction(V_f) and packing on the longitudinal tensile response.

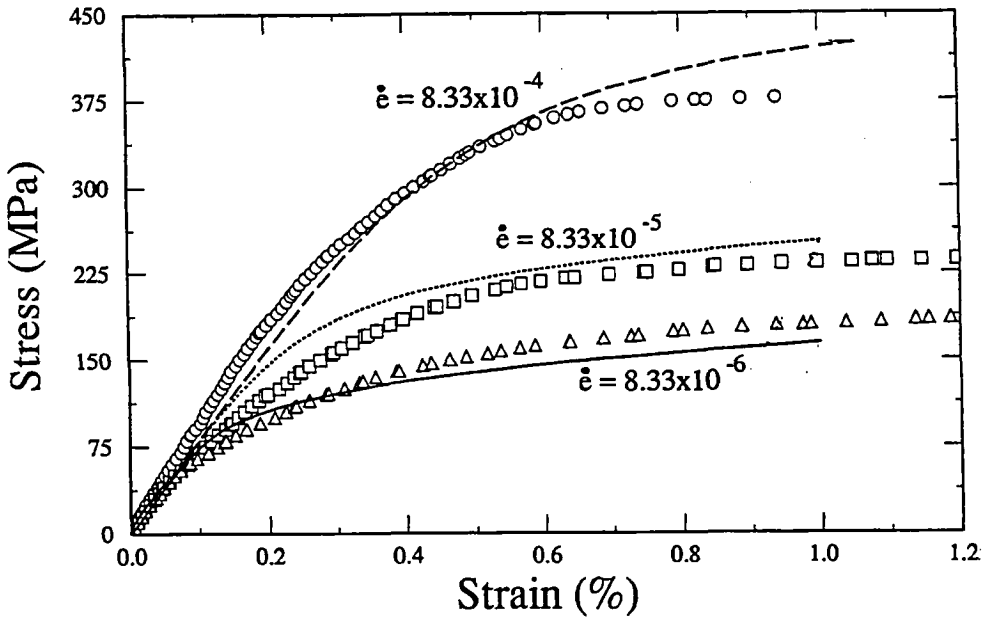

Figure 10: GVIPS correlation(lines) with experimental tensile data (symbols) at various total strain rates, see Arnold et al. (1994a).

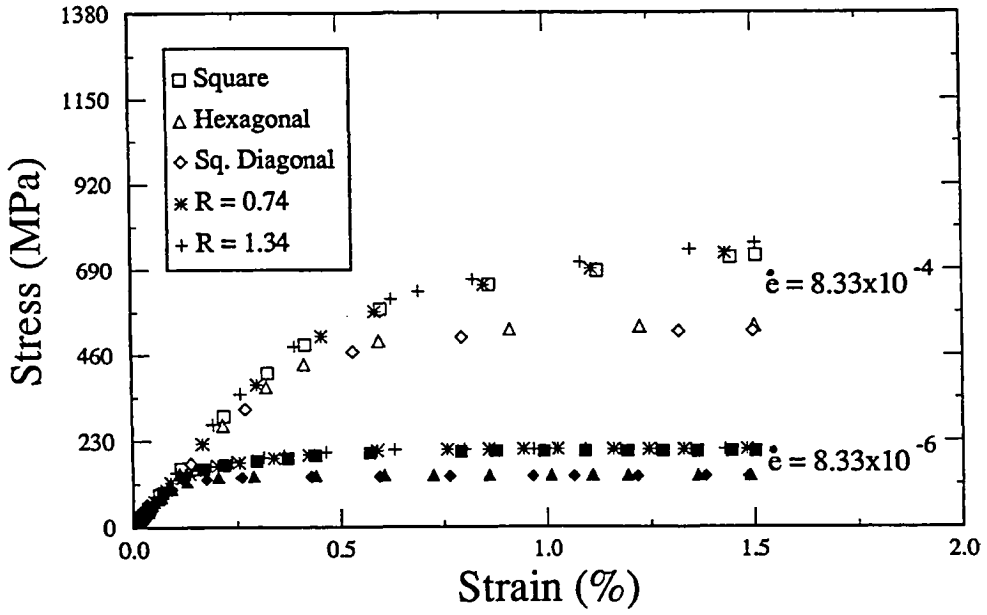

Figure 11: Influence of strain rate and fiber packing geometry on the transverse tensile response of a TMC system given a 35 percent fiber volume fraction.

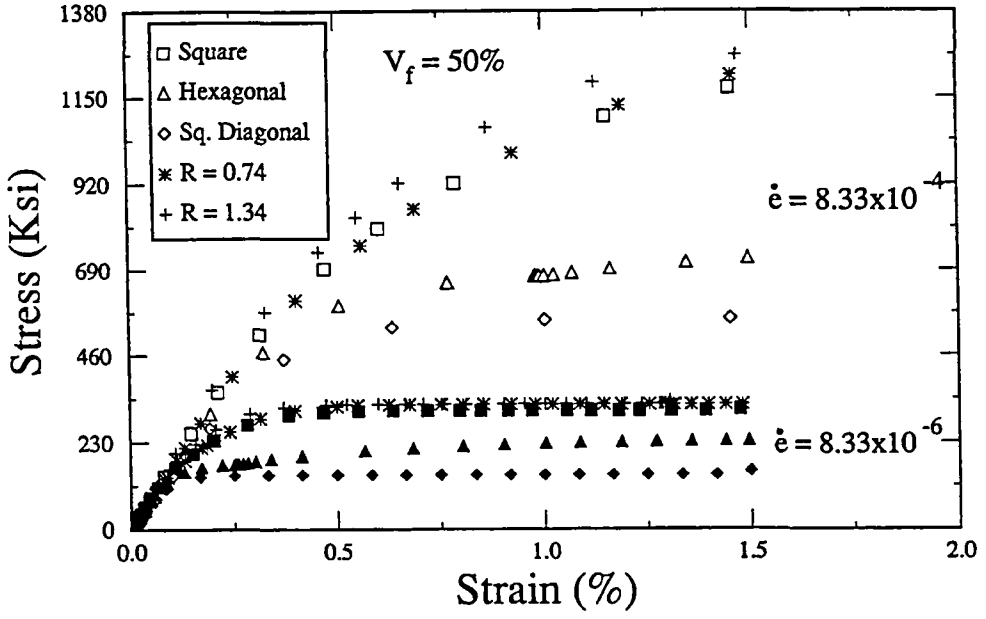

Figure 12: Influence of strain rate and fiber packing geometry on the transverse tensile response of a TMC system given a 50 percent fiber volume fraction.

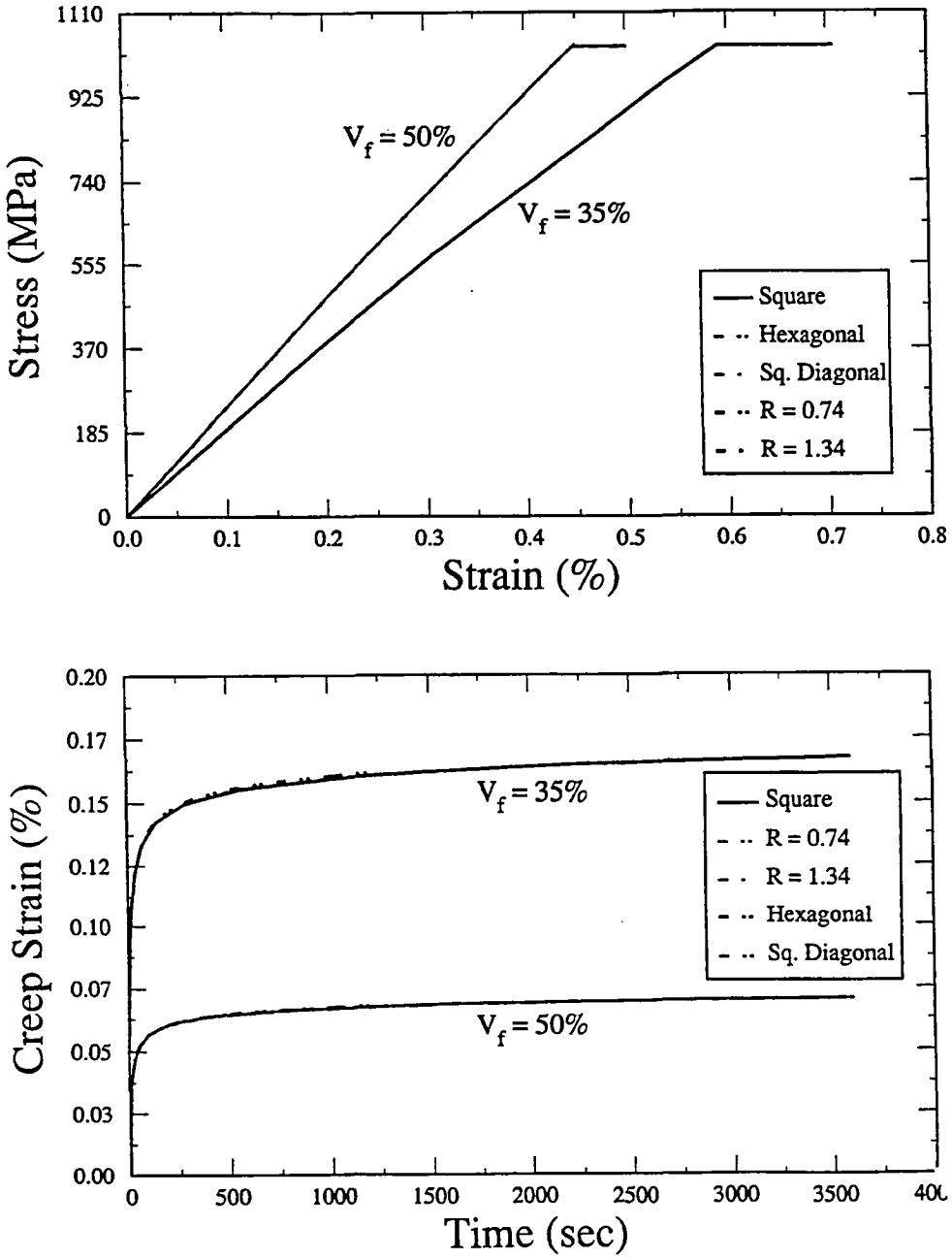

Figure 13: Influence of volume fraction and fiber packing geometry on the longitudinal creep response of a TMC system.

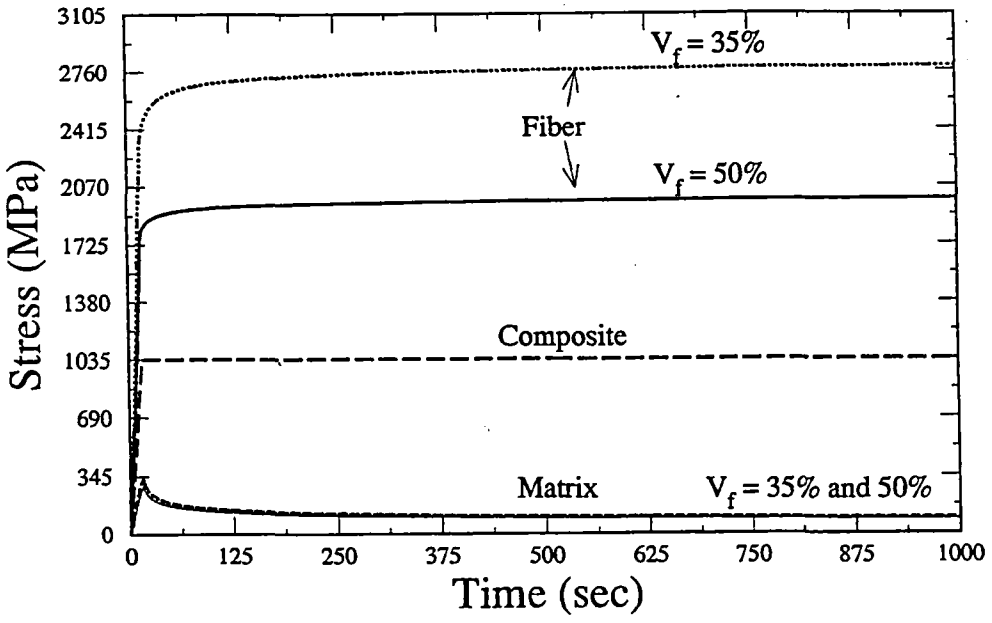

Figure 14: The longitudinal stress redistribution as function of time in the fiber, composite and matrix during the simulation of a longitudinal creep test.

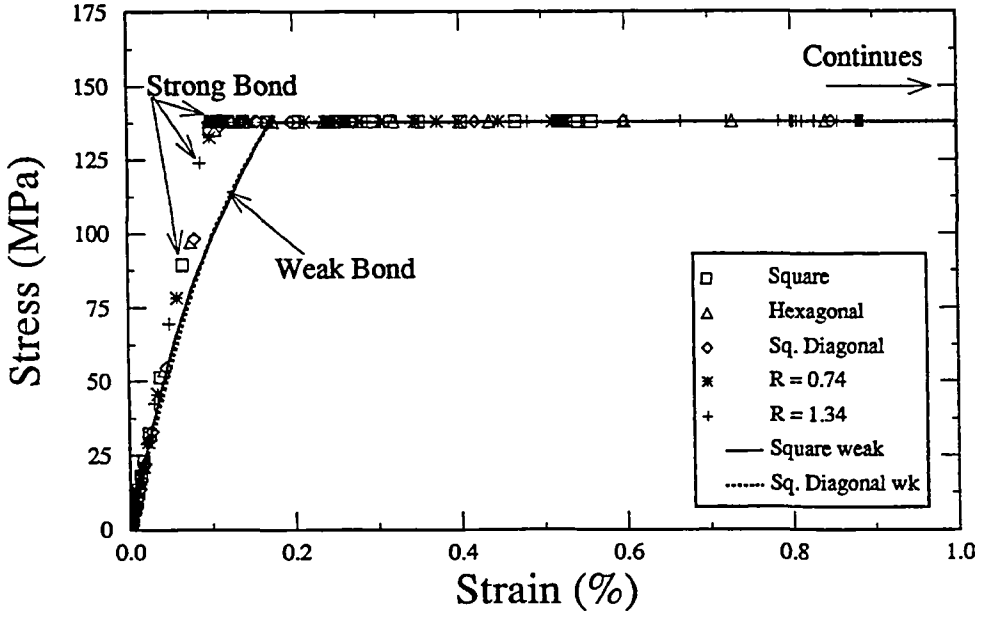

Figure 15: The transverse stress-strain response of a 35 percent volume fraction TMC system illustrating the influence of fiber packing geometry and bond strength on the transverse creep behavior, see Figs. 16 and 17.

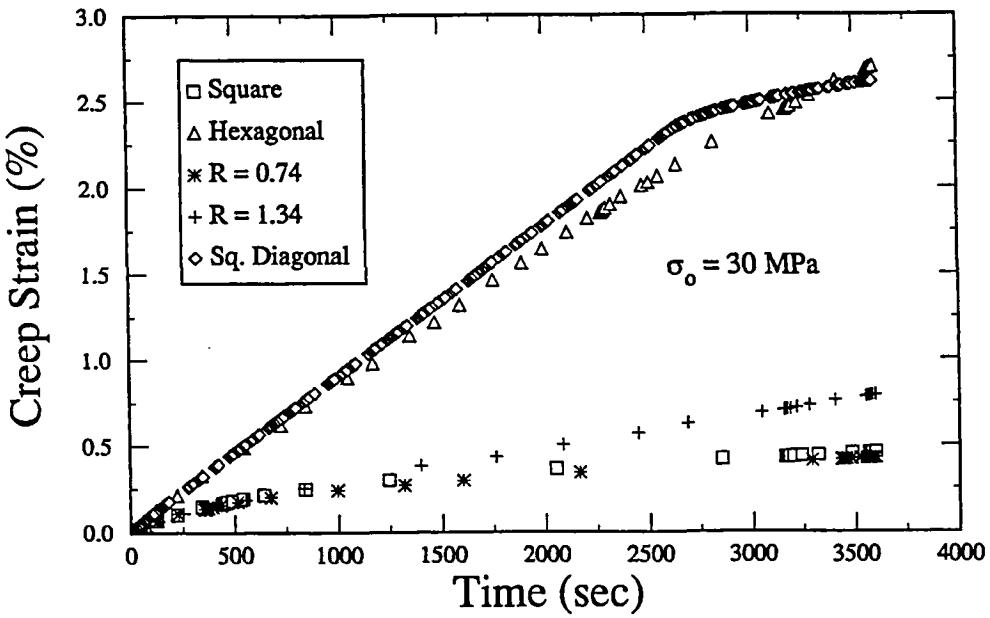

Figure 16: Illustrates the transverse creep strain versus time response of a strongly bonded, 35 percent fiber volume fraction TMC system for the five fiber packing geometries.

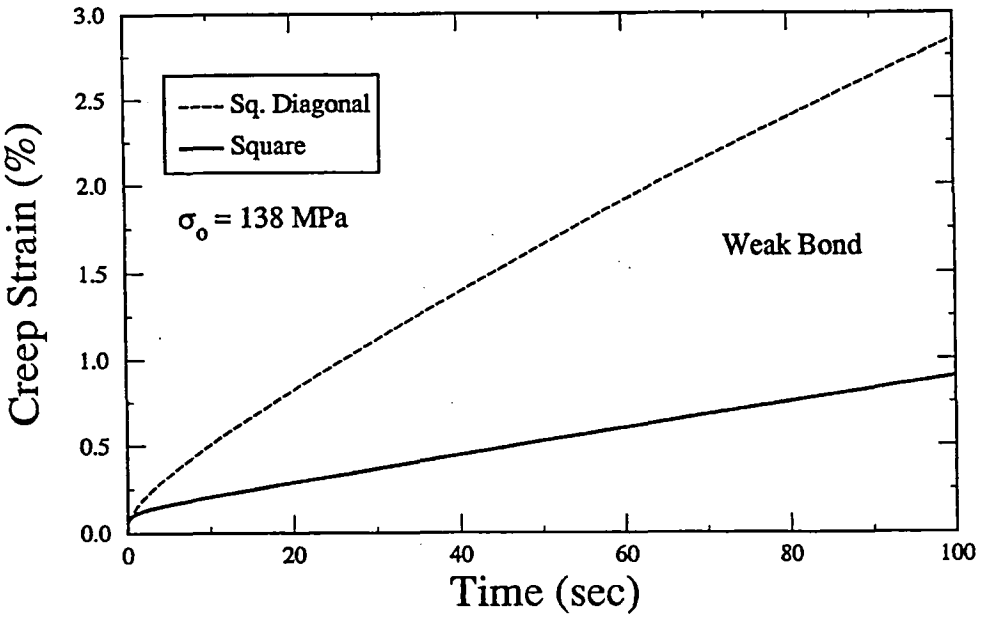

Figure 17: Illustrates the transverse creep strain versus time response of a weakly bonded, 35 percent fiber volume fraction TMC system for a square and square-diagonal fiber packing geometries.

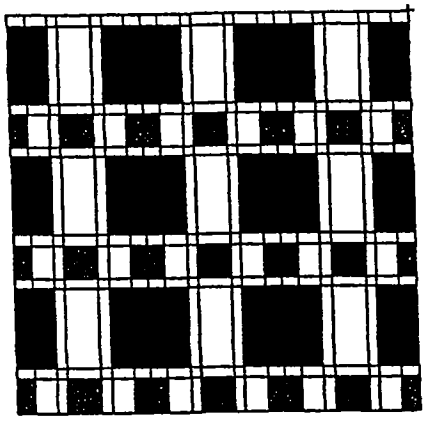

Hybrid array

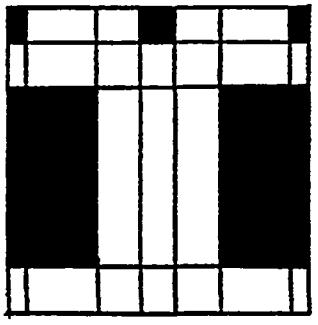

RVE

Figure 18: Schematic of a specific hybrid architecture involving large (weakly bonded) and small (strongly bonded) diameter fibers.

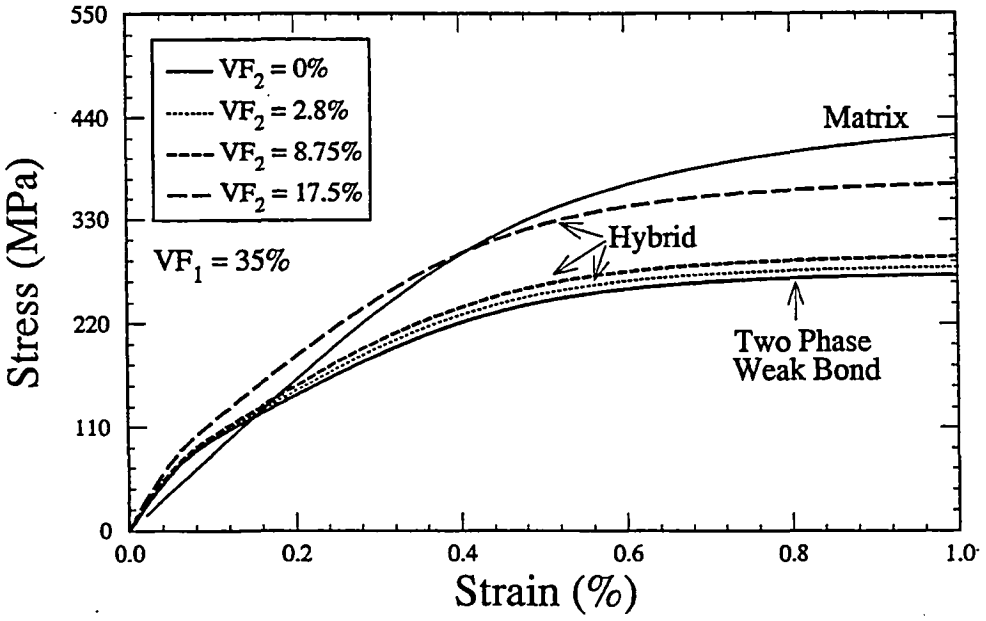

Figure 19: Influence of smaller diameter fiber volume fraction, for the specific hybrid architecture of Fig. 18, on the transverse composite tensile response.

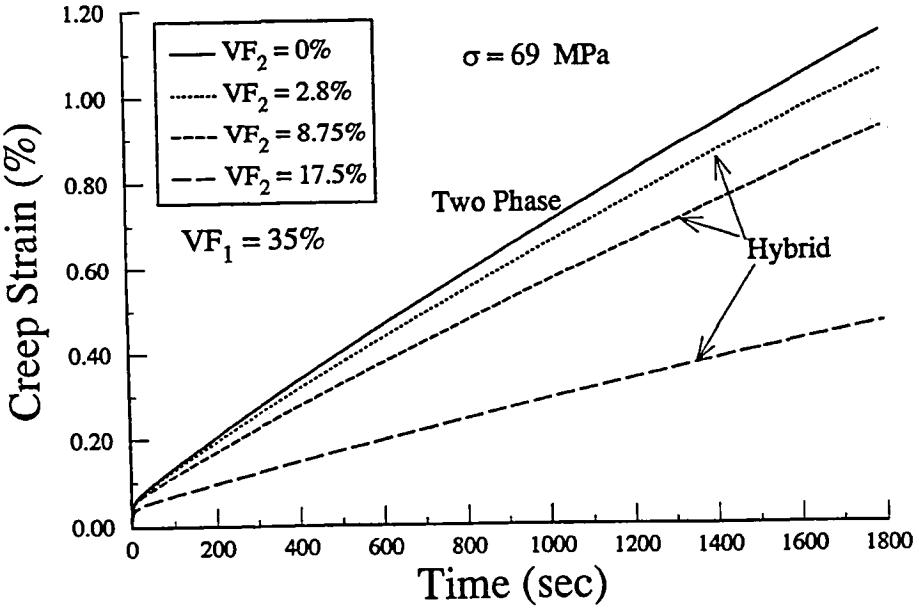

Figure 20: Influence of smaller diameter fiber volume fraction, for the specific hybrid architeture of Fig. 18, on the transverse composite creep response.

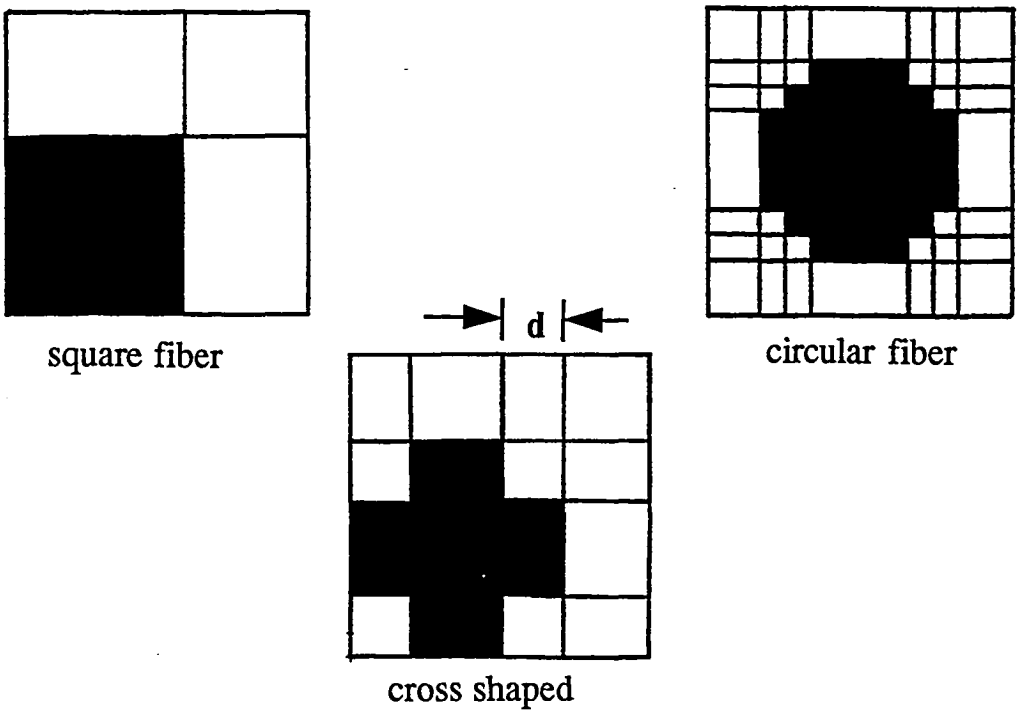

Figure 21: Schematic of a square, circular, and shallow and deep cross fiber cross section representative volume elements.

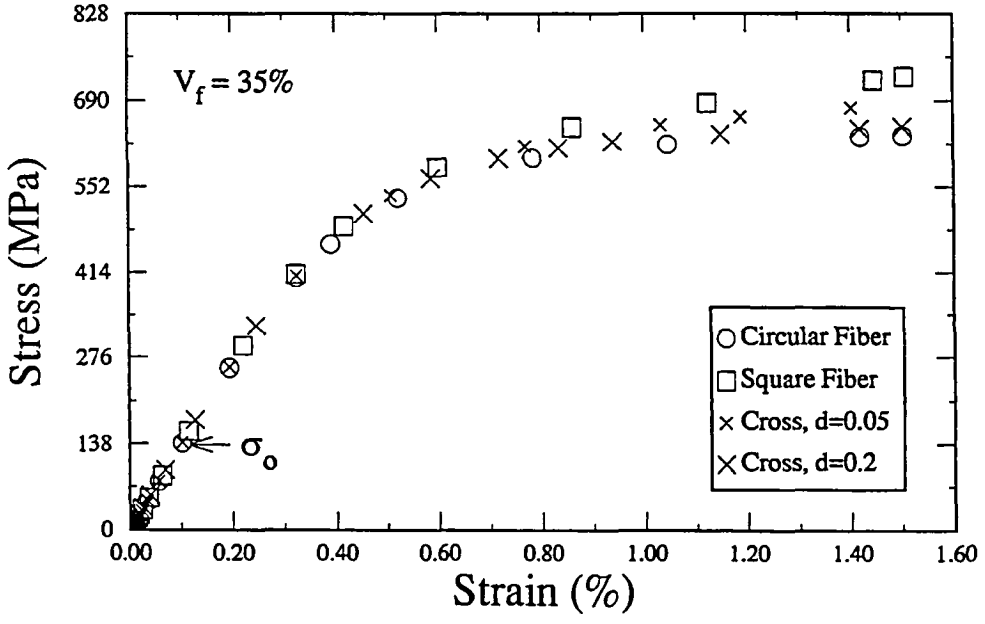

Figure 22: The stress versus strain response of a strongly bonded TMC system, illustrating the influence of fiber shape on the transverse tensile behavior.

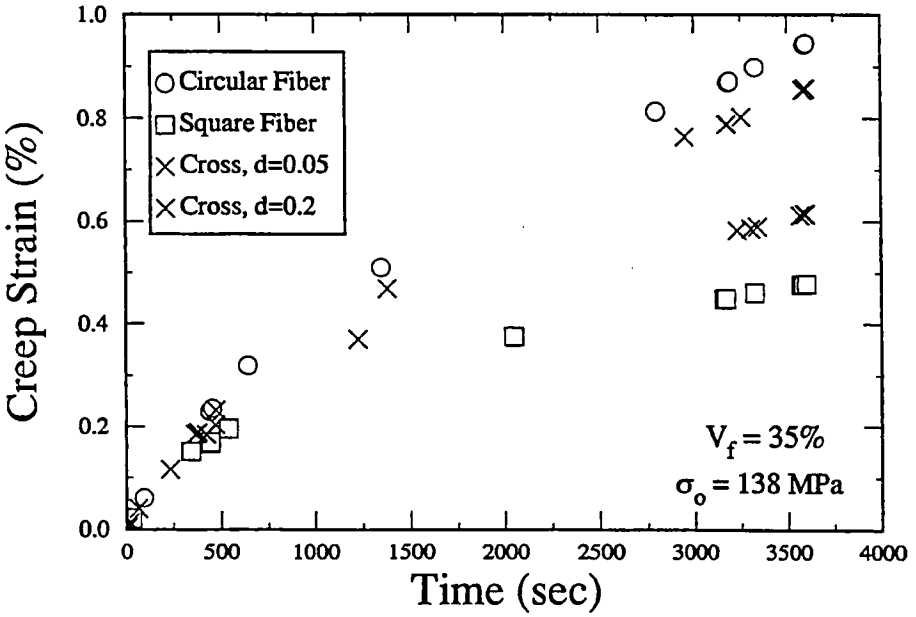

Figure 23: The transverse creep strain versus creep time response of a strongly bonded TMC system, illustrating the influence of fiber shape on the transverse creep behavior.

REPORT DOCUMENTATION PAGE

Form Approved
OMB No. 0704-0188

1. AGENCY USE ONLY (*Leave blank*)	2. REPORT DATE	3. REPORT TYPE AND DATES COVERED
	October 1995	Technical Memorandum

4. TITLE AND SUBTITLE

Influence of Fiber Architecture on the Elastic and Inelastic Response of Metal Matrix Composites

5. FUNDING NUMBERS

WU-505-63-12

6. AUTHOR(S)

Steven M. Arnold, Marek-Jerzy Pindera, and Thomas E. Wilt

7. PERFORMING ORGANIZATION NAME(S) AND ADDRESS(ES)

National Aeronautics and Space Administration
Lewis Research Center
Cleveland, Ohio 44135-3191

8. PERFORMING ORGANIZATION REPORT NUMBER

E-9067

9. SPONSORING/MONITORING AGENCY NAME(S) AND ADDRESS(ES)

National Aeronautics and Space Administration
Washington, D.C. 20546-0001

10. SPONSORING/MONITORING AGENCY REPORT NUMBER

NASA TM-106705

11. SUPPLEMENTARY NOTES

Steven M. Arnold, NASA Lewis Research Center; Marek-Jerzy Pindera, University of Virginia, Charlottesville, Virginia 22903 (work funded by NASA Grant NAG3-1377); and Thomas E. Wilt, University of Akron, Akron, Ohio 44235 (work funded by NASA Cooperative Agreement NCC3-368). Responsible person, Steven M. Arnold, organization code 5220, (216) 433-3334.

12a. DISTRIBUTION/AVAILABILITY STATEMENT

Unclassified - Unlimited
Subject Category 24

This publication is available from the NASA Center for Aerospace Information, (301) 621-0390.

12b. DISTRIBUTION CODE

13. ABSTRACT (*Maximum 200 words*)

This three part paper focuses on the effect of fiber architecture (i.e., shape and distribution) on the elastic and inelastic response of metal matrix composites. The first part provides an annotative survey of the literature, presented as a historical perspective, dealing with the effects of fiber shape and distribution on the response of advanced polymeric matrix and metal matrix composites. Previous investigations dealing with both continuously and discontinuously reinforced composites are included. A summary of the state-of-the-art will assist in defining new directions in this quickly reviving area of research. The second part outlines a recently developed analytical micromechanics model that is particularly well suited for studying the influence of these effects on the response of metal matrix composites. This micromechanics model, referred to as the generalized method of cells (GMC), is capable of predicting the overall, inelastic behavior of unidirectional, multi-phased composites given the properties of the constituents. In particular, the model is sufficiently general to predict the response of unidirectional composites reinforced by either continuous or discontinuous fibers with different inclusion shapes and spatial arrangements in the presence of either perfect or imperfect interfaces and/or interfacial layers. Recent developments regarding this promising model, as well as directions for future enhancements of the model's predictive capability, are included. Finally, the third part provides qualitative results generated using GMC for a representative titanium matrix composite system, SCS-6/TIMETAL 21S. Results are presented that correctly demonstrate the relative effects of fiber arrangement and shape on the longitudinal and transverse stress-strain and creep response, with both strong and weak fiber/matrix interfacial bonds. The fiber arrangements include square, square diagonal, hexagonal and rectangular periodic arrays, as well as a random array. The fiber shapes include circular, square and cross-shaped cross sections. The effect of fiber volume fraction on the observed stress-strain response is also discussed, as is the thus-far poorly documented strain rate sensitivity effect. In addition to the well documented features of architecture dependent response of continuously reinforced two-phase MMCs, new results involving continuous multi-phase internal architectures are presented. Specifically, stress-strain and creep response of composites with different size fibers having different internal arrangements and bond strengths are investigated with the aim of determining the feasibility of using this approach to enhance the transverse toughness and creep resistance of TMCs.

14. SUBJECT TERMS	15. NUMBER OF PAGES
Micromechanics; Strong bond; Weak bond viscoplasticity; Titanium matrix composite creep; Plasticity	69
	16. PRICE CODE: A04

17. SECURITY CLASSIFICATION OF REPORT	18. SECURITY CLASSIFICATION OF THIS PAGE	19. SECURITY CLASSIFICATION OF ABSTRACT	20. LIMITATION OF ABSTRACT
Unclassified	Unclassified	Unclassified	

National Aeronautics and
Space Administration

Lewis Research Center
21000 Brookpark Rd.
Cleveland, OH 44135-3191